

**Testing QCD factorization and charming penguin diagrams in charmless  $B \rightarrow PV$** R. Aleksan,<sup>1,\*</sup> P.-F. Giraud,<sup>1,†</sup> V. Morénas,<sup>2,‡</sup> O. Pène,<sup>3,§</sup> and A. S. Safir<sup>4,||</sup><sup>1</sup>DSM/DAPNIA/SPP, CEA/Saclay, F-91191 Gif-sur-Yvette, France<sup>2</sup>LPC, Université Blaise Pascal, CNRS/IN2P3 F-63000 Aubière Cedex, France<sup>3</sup>LPT (Bât.210), Université de Paris XI, Centre d'Orsay, 91405 Orsay-Cedex, France<sup>4</sup>LMU München, Sektion Physik, Theresienstraße 37, D-80333 München, Germany

(Received 26 January 2003; published 23 May 2003)

We try a global fit of the experimental branching ratios and  $CP$  asymmetries of the charmless  $B \rightarrow PV$  decays according to QCD factorization. We find it impossible to reach satisfactory agreement, the confidence level (C.L.) of the best fit being smaller than 0.1%. The main reason for this failure is the difficulty to accommodate several large experimental branching ratios of the strange channels. Furthermore, experiment was not able to exclude a large direct  $CP$  asymmetry in  $\overline{B^0} \rightarrow \rho^+ \pi^-$ , which is predicted to be very small by QCD factorization. Trying a fit with QCD factorization complemented by a charming-penguin-diagram-inspired model we reach a best fit which is not excluded by experiment (C.L. of about 8%) but is not fully convincing. These negative results must be tempered by the remark that some of the experimental data used are recent and might still evolve significantly.

DOI: 10.1103/PhysRevD.67.094019

PACS number(s): 13.25.Hw

**I. INTRODUCTION**

It is an important theoretical challenge to master the nonleptonic decay amplitudes and particularly  $B$  nonleptonic decay. It is not only important *per se*, in view of the many experimental branching ratios which have been measured recently with increasing accuracy by BaBar [1–10], Belle [11–15], and CLEO [16–21], but it is also necessary in order to get control over the measurement of  $CP$  violating parameters and particularly the so-called angle  $\alpha$  of the unitarity triangle. It is well known that extracting  $\alpha$  from measured indirect  $CP$  asymmetries needs a sufficient control of the relative size of the so-called tree ( $T$ ) and penguin ( $P$ ) amplitudes.

However, the theory of nonleptonic weak decays is a difficult issue. Lattice QCD gives predictions for semileptonic or purely leptonic decays but not directly for nonleptonic ones. For a while, one has used what is now called “naive factorization” which replaces the matrix element of a four-fermion operator in a heavy-quark decay by the product of the matrix elements of two currents, one semileptonic matrix element and one purely leptonic. It has been noticed for a while that naive factorization did provide reasonable results, although it was impossible to derive it rigorously from QCD except in the  $N_c \rightarrow \infty$  limit. It is also well known that the matrix elements computed via naive factorization have a wrong anomalous dimension.

Recently an important theoretical progress has been performed [22,23] which is commonly called “QCD factorization.” It is based on the fact that the  $b$  quark is heavy com-

pared to the intrinsic scale of strong interactions. This allows one to deduce that nonleptonic decay amplitudes in the heavy-quark limit have a simple structure. It implies that corrections termed “nonfactorizable,” which were thought to be intractable, can be calculated rigorously. The anomalous dimension of the matrix elements is now correct to the order at which the calculation is performed. Unluckily the subleading  $\mathcal{O}(\Lambda/m_b)$  contributions cannot in general be computed rigorously because of infrared singularities, and some of these which are chirally enhanced are not small, of order  $\mathcal{O}(m_\pi^2/m_b(m_u+m_d))$ , which shows that the inverse  $m_b$  power is compensated by  $m_\pi/(m_u+m_d)$ . In the seminal papers of [22,23], these contributions are simply bounded according to a qualitative argument which could as well justify a significantly larger bound with the risk of seeing these unpredictable terms become dominant. It is then of utmost importance to check experimentally QCD factorization (QCDF).

Since a few years, it has been applied to  $B \rightarrow PP$  (two charmless pseudoscalar mesons) decays. The general feature is that the decay to nonstrange final states is predicted to be slightly larger than experiment while the decay to strange final states is significantly underestimated. In [23] it is claimed that this can be cured by a value of the unitarity-triangle angle  $\gamma$  larger than generally expected, larger maybe than  $90^\circ$ . Taking also into account various uncertainties the authors conclude positively as for the agreement of QCD factorization with the data. In [24,25] it was objected that the large branching ratios for strange channels argued in favor of the presence of a specific nonperturbative contribution called “charming penguin diagrams” [25–30]. We will return to this approach later.

The  $B \rightarrow PV$  (charmless pseudoscalar + vector mesons) channels are more numerous and allow a more extensive check. In Ref. [31] it was shown that naive factorization implied a rather small  $|P|/|T|$  ratio, for the  $\overline{B^0} \rightarrow \rho^+ \pi^-$  decay channel, to be compared to the larger one for the  $B$

\*Email address: aleksan@hep.saclay.cea.fr

†Email address: giraudpf@hep.saclay.cea.fr

‡Email address: morenas@clermont.in2p3.fr

§Email address: pene@th.u-psud.fr

||Email address: safir@theorie.physik.uni-muenchen.de

$\rightarrow \pi^+ \pi^-$ . This prediction is still valid in QCD factorization where the  $|P|/|T|$  ratio is of about 3% (8%) for the  $\overline{B^0} \rightarrow \rho^+ \pi^-$  ( $\overline{B^0} \rightarrow \rho^- \pi^+$ ) channel against about 20% for the  $\overline{B^0} \rightarrow \pi^+ \pi^-$  one. If this prediction were reliable, it would put the  $\overline{B^0} \rightarrow \rho^+ \pi^-$  channel in a good position to measure the Cabibbo-Kobayashi-Maskawa (CKM) angle  $\alpha$  via indirect  $CP$  violation. This remark triggered the present work: we wanted to check QCD factorization in the  $B \rightarrow PV$  sector to estimate the chances for a relatively easy determination of the angle  $\alpha$ .

The noncharmed  $B \rightarrow PV$  amplitudes have been computed in naive factorization [32], in some extension of naive factorization including strong phases [33], in QCD factorization [34–36], and some of them in so-called perturbative QCD [37,38]. In [39], a global fit to  $B \rightarrow PP, PV, VV$  was investigated using QCDF in the heavy-quark limit and a plausible set of soft QCD parameters has been found that, apart from three pseudoscalar vector channels, fit well the experimental branching ratios. Recently [36] it was claimed from a global fit to  $B \rightarrow PP, PV$  that the predictions of QCD factorization are in good agreement with experiment when one excludes some channels from the global fit. When this paper appeared we had been for some time considering this question and our feeling was significantly less optimistic. This difference shows that the matter is far from trivial mainly because experimental uncertainties can still be open to some discussion. We would like in this paper to understand better the origin of the difference between our unpublished conclusion and the one presented in [36] and try to settle the present status of the comparison of QCD factorization with experiment.

One general remark about QCD factorization is that it yields predictions which do not differ so much from naive factorization ones. This is expected since QCD factorization makes a perturbative expansion the zeroth order of which being naive factorization. As a consequence, QCD factorization predicts very small direct  $CP$  violation in the nonstrange channels. Naive factorization predicts vanishing direct  $CP$  violation. Indeed, direct  $CP$  violation needs the occurrence of two distinct strong contributions with a strong phase between them. It vanishes when the subdominant strong contribution vanishes and also when the relative strong phase does as is the case in naive factorization. In the case of nonstrange decays, the penguin ( $P$ ) and tree ( $T$ ) contributions being at the same order in the Cabibbo angle, the penguin diagram is strongly suppressed because the Wilson coefficients are suppressed by at least one power of the strong coupling constant  $\alpha_s$  and the strong phase in QCD factorization is generated by a  $\mathcal{O}(\alpha_s)$  correction. Having both  $P/T$  and the strong phase small, the direct  $CP$  asymmetries are doubly suppressed. Therefore a sizable experimental direct  $CP$  asymmetry in  $\overline{B^0} \rightarrow \rho^+ \pi^-$  which is not excluded by experiment [9] would be at odds with QCD factorization. We will discuss this later on. Notice that this argument is independent of the value of the unitarity angle  $\gamma$ , contrarily to arguments based on the value of some branching ratios which depend on  $\gamma$  [23].

The perturbative QCD (PQCD) predicts larger direct  $CP$

asymmetries than QCDF due to the fact that penguin contributions to annihilation diagrams, claimed to be calculable in PQCD, contribute to a larger amount to the amplitude and have a large strong phase. In fact, in PQCD, this penguin annihilation diagram is claimed to be of the same order,  $\mathcal{O}(\alpha_s)$ , than the dominant naive factorization diagram while in QCDF it is also  $\mathcal{O}(\alpha_s)$  but smaller than the dominant naive factorization which is  $\mathcal{O}(1)$ . Hence, in PQCD, this large penguin contribution with a large strong phase yields a large  $CP$  asymmetry [40–42].

If QCD factorization is concluded to be unable to describe the present data satisfactorily, while there is to our knowledge no theoretical argument against it, we have to incriminate nonperturbative contributions which are larger than expected. One could simply enlarge the allowed bound for those contributions which are formally subleading but might be large. However, a simple factor of 2 on these bounds makes these unpredictable contributions comparable in size with the predictable ones, if not larger. This spoils the predictivity of the whole program.

A second line is to make some model about the nonperturbative contribution. The “charming penguin diagram” approach [27,30] starts from noticing the underestimate of strange-channel branching ratios by the factorization approaches. This will be shown to apply to the  $PV$  channels as well as to the  $PP$  ones. This has triggered us to try a charming-penguin-diagram-inspired approach. It is assumed that some hadronic contribution to the penguin loop is nonperturbative, in other words that weak interactions create a charm-anticharm intermediate state which turns into non-charmed final states by strong rescattering. In order to make the model as predictive as possible we will use not more than two unknown complex numbers and use flavor symmetry in strong rescattering.

In Sec. II we will recall the weak-interaction effective Hamiltonian. In Sec. III we will recall QCD factorization. In Sec. IV we will compare QCD factorization with experimental branching ratios and direct  $CP$  asymmetries. In Sec. V we will propose a model for nonperturbative contribution and compare it to experiment. We will then conclude.

## II. EFFECTIVE HAMILTONIAN

The effective weak Hamiltonian for charmless hadronic  $B$  decays consists of a sum of local operators  $\mathcal{Q}_i$  multiplied by short-distance coefficients  $C_i$  given in Table I and products of elements of the quark mixing matrix,  $\lambda_p = V_{pb} V_{ps}^*$  or  $\lambda'_p = V_{pb} V_{pd}^*$ . Below we will focus on  $B \rightarrow PV$  decays, where  $P$  and  $V$  hold for pseudoscalar and vector mesons, respectively. Using the unitarity relation  $-\lambda_t = \lambda_u + \lambda_c$ , we write

$$\mathcal{H}_{\text{eff}} = \frac{G_F}{\sqrt{2}} \sum_{p=u,c} \lambda_p \left( C_1 \mathcal{Q}_1^p + C_2 \mathcal{Q}_2^p + \sum_{i=3,\dots,10} C_i \mathcal{Q}_i + C_{7\gamma} \mathcal{Q}_{7\gamma} + C_{8g} \mathcal{Q}_{8g} \right) + \text{H.c.}, \quad (1)$$

where  $\mathcal{Q}_{1,2}^p$  are the left-handed current-current operators arising from  $W$ -boson exchange,  $\mathcal{Q}_{3,\dots,6}$  and  $\mathcal{Q}_{7,\dots,10}$  are

TABLE I. Wilson coefficients  $C_i$  in the NDR scheme. Input parameters are  $\Lambda_{\overline{\text{MS}}}^{(5)}=0.225$  GeV,  $m_t(m_t)=167$  GeV,  $m_b(m_b)=4.2$  GeV,  $M_W=80.4$  GeV,  $\alpha=1/129$ , and  $\sin^2\theta_W=0.23$  [23].

NLO	$C_1$	$C_2$	$C_3$	$C_4$	$C_5$	$C_6$
$\mu=m_b/2$	1.137	-0.295	0.021	-0.051	0.010	-0.065
$\mu=m_b$	1.081	-0.190	0.014	-0.036	0.009	-0.042
$\mu=2m_b$	1.045	-0.113	0.009	-0.025	0.007	-0.027
	$C_7/\alpha$	$C_8/\alpha$	$C_9/\alpha$	$C_{10}/\alpha$	$C_{7\gamma}^{\text{eff}}$	$C_{8g}^{\text{eff}}$
$\mu=m_b/2$	-0.024	0.096	-1.325	0.331	—	—
$\mu=m_b$	-0.011	0.060	-1.254	0.223	—	—
$\mu=2m_b$	0.011	0.039	-1.195	0.144	—	—
LO	$C_1$	$C_2$	$C_3$	$C_4$	$C_5$	$C_6$
$\mu=m_b/2$	1.185	-0.387	0.018	-0.038	0.010	-0.053
$\mu=m_b$	1.117	-0.268	0.012	-0.027	0.008	-0.034
$\mu=2m_b$	1.074	-0.181	0.008	-0.019	0.006	-0.022
	$C_7/\alpha$	$C_8/\alpha$	$C_9/\alpha$	$C_{10}/\alpha$	$C_{7\gamma}^{\text{eff}}$	$C_{8g}^{\text{eff}}$
$\mu=m_b/2$	-0.012	0.045	-1.358	0.418	-0.364	-0.169
$\mu=m_b$	-0.001	0.029	-1.276	0.288	-0.318	-0.151
$\mu=2m_b$	0.018	0.019	-1.212	0.193	-0.281	-0.136

QCD and electroweak penguin operators, and  $Q_{7\gamma}$  and  $Q_{8g}$  are the electromagnetic and chromomagnetic dipole operators. They are given by

$$Q_1^p = (\bar{p}b)_{V-A}(\bar{s}p)_{V-A}, \quad Q_2^p = (\bar{p}_i b_j)_{V-A}(\bar{s}_j p_i)_{V-A},$$

$$Q_3 = (\bar{s}b)_{V-A} \sum_q (\bar{q}q)_{V-A},$$

$$Q_4 = (\bar{s}_i b_j)_{V-A} \sum_q (\bar{q}_j q_i)_{V-A},$$

$$Q_5 = (\bar{s}b)_{V-A} \sum_q (\bar{q}q)_{V+A},$$

$$Q_6 = (\bar{s}_i b_j)_{V-A} \sum_q (\bar{q}_j q_i)_{V+A},$$

$$Q_7 = (\bar{s}b)_{V-A} \sum_q \frac{3}{2} e_q (\bar{q}q)_{V+A},$$

$$Q_8 = (\bar{s}_i b_j)_{V-A} \sum_q \frac{3}{2} e_q (\bar{q}_j q_i)_{V+A},$$

$$Q_9 = (\bar{s}b)_{V-A} \sum_q \frac{3}{2} e_q (\bar{q}q)_{V-A},$$

$$Q_{10} = (\bar{s}_i b_j)_{V-A} \sum_q \frac{3}{2} e_q (\bar{q}_j q_i)_{V-A},$$

$$Q_{7\gamma} = \frac{-e}{8\pi^2} m_b \bar{s} \sigma_{\mu\nu} (1 + \gamma_5) F^{\mu\nu} b,$$

$$Q_{8g} = \frac{-g_s}{8\pi^2} m_b \bar{s} \sigma_{\mu\nu} (1 + \gamma_5) G^{\mu\nu} b, \quad (2)$$

where  $(\bar{q}_1 q_2)_{V\pm A} = \bar{q}_1 \gamma_\mu (1 \pm \gamma_5) q_2$ ,  $i, j$  are color indices,  $e_q$  are the electric charges of the quarks in units of  $|e|$ , and a summation over  $q = u, d, s, c, b$  is implied. The definition of the dipole operators  $Q_{7\gamma}$  and  $Q_{8g}$  corresponds to the sign convention  $iD^\mu = i\partial^\mu + g_s A_a^\mu t_a$  for the gauge-covariant derivative. The Wilson coefficients are calculated at a high scale  $\mu \sim M_W$  and evolved down to a characteristic scale  $\mu \sim m_b$  using next-to-leading order renormalization-group equations. The essential problem obstructing the calculation of nonleptonic decay amplitudes resides in the evaluation of the hadronic matrix elements of the local operators contained in the effective Hamiltonian.

### III. QCD FACTORIZATION IN $B \rightarrow PV$ DECAYS

When the QCDF method is applied to the decays  $B \rightarrow PV$ , the hadronic matrix elements of the local effective operators can be written as

$$\langle PV | \mathcal{O}_i | B \rangle = F_1^{B \rightarrow P}(0) T_{V,i}^I \star f_V \Phi_V + A_0^{B \rightarrow V}(0) T_{P,i}^I \star f_P \Phi_P + T_i^{\text{II}} \star f_B \Phi_B \star f_V \Phi_V \star f_P \Phi_P, \quad (3)$$

where  $\Phi_M$  are leading-twist light-cone distribution amplitudes, and the  $\star$ -products imply an integration over the light-cone momentum fractions of the constituent quarks inside the mesons. A graphical representation of this result is shown in Fig. 1.

Here  $F_1^{B \rightarrow P}$  and  $A_0^{B \rightarrow V}$  denote the form factors for  $B \rightarrow P$  and  $B \rightarrow V$  transitions, respectively.  $\Phi_B(\xi)$ ,  $\Phi_V(x)$ , and  $\Phi_P(y)$  are the light-cone distribution amplitudes (LCDAs) of

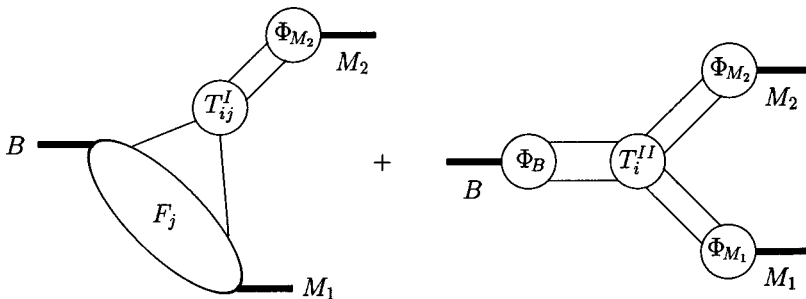


FIG. 1. Graphical representation of the factorization formula. Only one of the two form-factor terms in Eq. (3) is shown for simplicity.

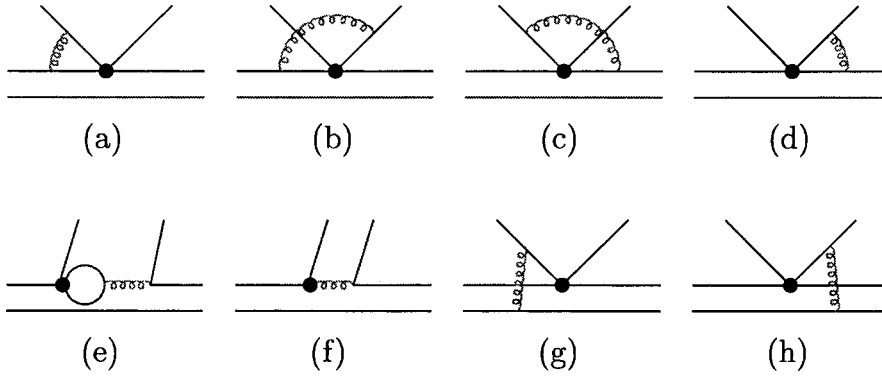


FIG. 2. Order  $\alpha_s$  corrections to the hard-scattering kernels. The upward quark lines represent the emitted mesons from  $b$  quark weak decays. These diagrams are commonly called vertex corrections, penguin corrections, and hard-spectator-scattering diagrams for (a)–(d), (e),(f), and (g),(h), respectively.

valence quark Fock states for  $B$ , vector, and pseudoscalar mesons, respectively.  $T_i^{I,II}$  denote the hard-scattering kernels, which are dominated by hard gluon exchange when the power suppressed  $\mathcal{O}(\Lambda_{QCD}/m_b)$  terms are neglected. So they are calculable order by order in perturbation theory. The leading terms of  $T^I$  come from the tree level and correspond to the naive factorization (NF) approximation. The order of  $\alpha_s$  terms of  $T^I$  can be depicted by vertex-correction diagrams Figs. 2(a)–2(d) and penguin-correction diagrams Figs. 2(e),(f).  $T^{II}$  describes the hard interactions between the spectator quark and the emitted meson  $M_2$  when the gluon virtuality is large. Its lowest order terms are  $\mathcal{O}(\alpha_s)$  and can be depicted by hard-spectator-scattering diagrams, Figs. 2(g)–2(h). One of the most interesting results of the QCDF approach is that, in the heavy-quark limit, the strong phases arise naturally from the hard-scattering kernels at the order of  $\alpha_s$ . As for the nonperturbative part, they are, as already mentioned, taken into account by the form factors and the LCDAs of mesons up to corrections which are power suppressed in  $1/m_b$ .

With the above discussions on the effective Hamiltonian of  $B$  decays Eq. (1) and the QCDF expressions of hadronic matrix elements, Eq. (3), the decay amplitudes for  $B \rightarrow PV$  in the heavy-quark limit can be written as

$$A(B \rightarrow PV) = \frac{G_F}{\sqrt{2}} \sum_{p=u,c} \sum_{i=1}^{10} \lambda_p a_i^p \langle PV | \mathcal{O}_i | B \rangle_{nf}. \quad (4)$$

The above  $\langle PV | \mathcal{O}_i | B \rangle_{nf}$  are the factorized hadronic matrix elements, which have the same definitions as those in the NF approach. The “nonfactorizable” effects are included in the coefficients  $a_i$  which are process dependent. The coefficients  $a_i$  are collected in Sec. III A, and the explicit expressions for the decay amplitudes of  $B \rightarrow PV$  can be found in Appendix A.

According to the arguments in [22], the contributions of weak annihilation to the decay amplitudes are power suppressed, and they do not appear in the QCDF formula, Eq.

(3). But as emphasized in [40–42], the contributions from weak annihilation could give large strong phases with QCD corrections, and hence large  $CP$  violation could be expected, so their effects cannot simply be neglected. However, in the QCDF method, the annihilation topologies (see Fig. 3) violate factorization because of the end-point divergence. There is similar end-point divergence when considering the chirally enhanced hard-spectator scattering. One possible way is to treat the endpoint divergence from different sources as different phenomenological parameters [23]. The corresponding price is the introduction of model dependence and extra numerical uncertainties in the decay amplitudes. In this work, we will follow the treatment of Ref. [23] and express the weak annihilation topological decay amplitudes as

$$A^a(B \rightarrow PV) \propto f_B f_P f_V \sum \lambda_p b_i, \quad (5)$$

where the parameters  $b_i$  are collected in Sec. III B, and the expressions for the weak annihilation decay amplitudes of  $B \rightarrow PV$  are listed in Appendix B.

### A. QCD coefficients $a_i$

We express the QCD coefficients  $a_i$  [see Eq. (4)] in two parts: i.e.,  $a_i = a_{i,I} + a_{i,II}$ . The first term  $a_{i,I}$  contains the naive factorization and the vertex corrections which are described by Figs. 2(a)–2(f), while the second part  $a_{i,II}$  corresponds to the hard-spectator-scattering diagrams Figs. 2(g),(h).

There are two different cases according to the final states. Case I is that the recoiled meson  $M_1$  is a vector meson, and the emitted meson  $M_2$  corresponds to a pseudoscalar meson, and vice versa for case II. For case I, we sum up the results for  $a_i$  as follows:

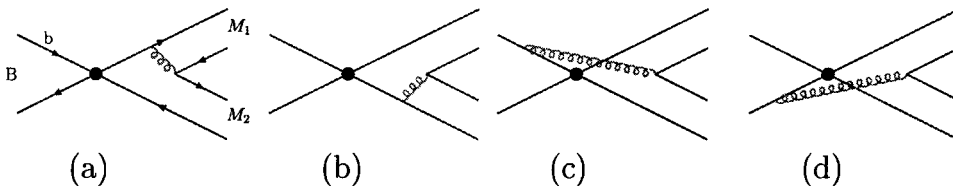


FIG. 3. Order  $\alpha_s$  corrections to the weak annihilations of charmless decays  $B \rightarrow PV$ .

$$a_{1,I} = C_1 + \frac{C_2}{N_c} \left[ 1 + \frac{C_F \alpha_s}{4\pi} V_M \right], \quad a_{10,II} = \frac{\pi C_F \alpha_s}{N_c^2} C_9 H(BM_1, M_2), \quad (6)$$

$$a_{1,II} = \frac{\pi C_F \alpha_s}{N_c^2} C_2 H(BM_1, M_2),$$

$$a_{2,I} = C_2 + \frac{C_1}{N_c} \left[ 1 + \frac{C_F \alpha_s}{4\pi} V_M \right],$$

$$a_{2,II} = \frac{\pi C_F \alpha_s}{N_c^2} C_1 H(BM_1, M_2),$$

$$a_{3,I} = C_3 + \frac{C_4}{N_c} \left[ 1 + \frac{C_F \alpha_s}{4\pi} V_M \right],$$

$$a_{3,II} = \frac{\pi C_F \alpha_s}{N_c^2} C_4 H(BM_1, M_2),$$

$$a_{4,I}^p = C_4 + \frac{C_3}{N_c} \left[ 1 + \frac{C_F \alpha_s}{4\pi} V_M \right] + \frac{C_F \alpha_s}{4\pi} \frac{P_{M,2}^p}{N_c},$$

$$a_{4,II} = \frac{\pi C_F \alpha_s}{N_c^2} C_3 H(BM_1, M_2),$$

$$a_{5,I} = C_5 + \frac{C_6}{N_c} \left[ 1 - \frac{C_F \alpha_s}{4\pi} V'_M \right],$$

$$a_{5,II} = -\frac{\pi C_F \alpha_s}{N_c^2} C_6 H'(BM_1, M_2),$$

$$a_{6,I}^p = C_6 + \frac{C_5}{N_c} \left[ 1 - 6 \frac{C_F \alpha_s}{4\pi} \right] + \frac{C_F \alpha_s}{4\pi} \frac{P_{M,3}^p}{N_c},$$

$$a_{6,II} = 0, \quad a_{7,I} = C_7 + \frac{C_8}{N_c} \left[ 1 - \frac{C_F \alpha_s}{4\pi} V'_M \right],$$

$$a_{7,II} = -\frac{\pi C_F \alpha_s}{N_c^2} C_8 H'(BM_1, M_2),$$

$$a_{8,I}^p = C_8 + \frac{C_7}{N_c} \left[ 1 - 6 \frac{C_F \alpha_s}{4\pi} \right] + \frac{\alpha}{9\pi} \frac{P_{M,3}^{p,ew}}{N_c},$$

$$a_{8,II} = 0, \quad a_{9,I} = C_9 + \frac{C_{10}}{N_c} \left[ 1 + \frac{C_F \alpha_s}{4\pi} V_M \right],$$

$$a_{9,II} = \frac{\pi C_F \alpha_s}{N_c^2} C_{10} H(BM_1, M_2),$$

$$a_{10,I}^p = C_{10} + \frac{C_9}{N_c} \left[ 1 + \frac{C_F \alpha_s}{4\pi} V_M \right] + \frac{\alpha}{9\pi} \frac{P_{M,2}^{p,ew}}{N_c},$$

where  $C_F = (N_c^2 - 1)/2N_c$ , and  $N_c = 3$ . The vertex parameters  $V_M$  and  $V'_M$  result from Figs. 2(a)–2(d); the QCD penguin parameters  $P_{M,i}^p$  and the electroweak penguin parameters  $P_{M,i}^{p,ew}$  result from Figs. 2(e)–2(f).

The vertex corrections are given by

$$V_M = 12 \ln \frac{m_b}{\mu} - 18 + \int_0^1 dx g(x) \Phi_M(x),$$

$$V'_M = 12 \ln \frac{m_b}{\mu} - 6 + \int_0^1 dx g(1-x) \Phi_M(x),$$

$$g(x) = 3 \left( \frac{1-2x}{1-x} \ln x - i\pi \right) + \left[ 2 \text{Li}_2(x) - \ln^2 x + \frac{2 \ln x}{1-x} - (3+2i\pi) \ln x - (x \leftrightarrow 1-x) \right], \quad (7)$$

where  $\text{Li}_2(x)$  is the dilogarithm function, whereas the constants 18 and 6 are specific to the naive dimensional reduction (NDR) scheme.

The penguin contributions are

$$\begin{aligned} P_{M,2}^p &= C_1 \left[ \frac{4}{3} \ln \frac{m_b}{\mu} + \frac{2}{3} - G_M(s_p) \right] + \left( C_3 - \frac{1}{2} C_9 \right) \\ &\quad \times \left[ \frac{8}{3} \ln \frac{m_b}{\mu} + \frac{4}{3} - G_M(0) - G_M(1) \right] \\ &\quad + \sum_{q=q'} \left( C_4 + C_6 + \frac{3}{2} e_q C_8 + \frac{3}{2} e_q C_{10} \right) \\ &\quad \times \left[ \frac{4}{3} \ln \frac{m_b}{\mu} - G_M(s_q) \right] - 2 C_{8g}^{\text{eff}} \int_0^1 dx \frac{\Phi_M(x)}{1-x}, \end{aligned}$$

$$\begin{aligned} P_{M,3}^p &= C_1 \left[ \frac{4}{3} \ln \frac{m_b}{\mu} + \frac{2}{3} - \hat{G}_M(s_p) \right] + \left( C_3 - \frac{1}{2} C_9 \right) \\ &\quad \times \left[ \frac{8}{3} \ln \frac{m_b}{\mu} + \frac{4}{3} - \hat{G}_M(0) - \hat{G}_M(1) \right] \\ &\quad + \sum_{q=q'} \left( C_4 + C_6 + \frac{3}{2} e_q C_8 + \frac{3}{2} e_q C_{10} \right) \\ &\quad \times \left[ \frac{4}{3} \ln \frac{m_b}{\mu} - \hat{G}_M(s_q) \right] - 2 C_{8g}^{\text{eff}}, \quad (8) \end{aligned}$$

and the electroweak penguin parameters  $P_{M,i}^{p,ew}$ ,

$$\begin{aligned}
P_{M,2}^{p,ew} &= (C_1 + N_c C_2) \left[ \frac{4}{3} \ln \frac{m_b}{\mu} + \frac{2}{3} - G_M(s_p) \right] - (C_3 + N_c C_4) \\
&\quad \times \left[ \frac{4}{3} \ln \frac{m_b}{\mu} + \frac{2}{3} - \frac{1}{2} G_M(0) - \frac{1}{2} G_M(1) \right] \\
&\quad + \sum_{q=q'} (N_c C_3 + C_4 + N_c C_5 + C_6) \\
&\quad \times \frac{3}{2} e_q \left[ \frac{4}{3} \ln \frac{m_b}{\mu} - G_M(s_q) \right] - N_c C_{7\gamma}^{\text{eff}} \int_0^1 dx \frac{\Phi_M(x)}{1-x}, \\
P_{M,3}^{p,ew} &= (C_1 + N_c C_2) \left[ \frac{4}{3} \ln \frac{m_b}{\mu} + \frac{2}{3} - \hat{G}_M(s_p) \right] - (C_3 + N_c C_4) \\
&\quad \times \left[ \frac{4}{3} \ln \frac{m_b}{\mu} + \frac{2}{3} - \frac{1}{2} \hat{G}_M(0) - \frac{1}{2} \hat{G}_M(1) \right] \\
&\quad + \sum_{q=q'} (N_c C_3 + C_4 + N_c C_5 + C_6) \\
&\quad \times \frac{3}{2} e_q \left[ \frac{4}{3} \ln \frac{m_b}{\mu} - \hat{G}_M(s_q) \right] - N_c C_{7\gamma}^{\text{eff}}, \tag{9}
\end{aligned}$$

where  $s_q = m_q^2/m_b^2$ , and where  $q'$  in the expressions for  $P_{M,i}^p$  and  $P_{M,i}^{p,ew}$  runs over all the active quarks at the scale  $\mu = \mathcal{O}(m_b)$ , i.e.,  $q' = u, d, s, c, b$ . The functions  $G_M(s)$  and  $\hat{G}_M(s)$  are given, respectively, by

$$G_M(s) = \int_0^1 dx G(s - i\epsilon, 1-x) \Phi_M(x), \tag{10}$$

$$\hat{G}_M(s) = \int_0^1 dx G(s - i\epsilon, 1-x) \Phi_M^p(x), \tag{11}$$

$$\begin{aligned}
G(s, x) &= -4 \int_0^1 du u(1-u) \ln[s - u(1-u)x] \\
&= \frac{2(12s + 5x - 3x \ln s)}{9x} \\
&\quad - \frac{4\sqrt{4s-x}(2s+x)}{3x^{3/2}} \arctan \sqrt{\frac{x}{4s-x}}. \tag{12}
\end{aligned}$$

The parameters  $H(BM_1, M_2)$  and  $H'(BM_1, M_2)$  in  $a_{i,II}$ , which originate from hard gluon exchanges between the spectator quark and the emitted meson  $M_2$ , are written as

$$\begin{aligned}
H(BV, P) &= \frac{f_B f_V}{m_B^2 A_0^{B \rightarrow V}(0)} \int_0^1 d\xi \int_0^1 dx \\
&\quad \times \int_0^1 dy \frac{\Phi_B(\xi)}{\xi} \frac{\Phi_P(x)}{\bar{x}} \frac{\Phi_V(y)}{\bar{y}},
\end{aligned}$$

$$\begin{aligned}
H'(BV, P) &= \frac{f_B f_V}{m_B^2 A_0^{B \rightarrow V}(0)} \int_0^1 d\xi \int_0^1 dx \\
&\quad \times \int_0^1 dy \frac{\Phi_B(\xi)}{\xi} \frac{\Phi_P(x)}{x} \frac{\Phi_V(y)}{\bar{y}}. \tag{13}
\end{aligned}$$

For case II (vector meson emitted) except for the parameters of  $H(BM_1, M_2)$  and  $H'(BM_1, M_2)$ , the expressions for  $a_i$  are similar to those in case I. However, we would like to point out that, because  $\langle V | (\bar{q}q)_{S \pm P} | 0 \rangle = 0$ , the contributions of the effective operators  $\mathcal{O}_{6,8}$  to the hadronic matrix elements vanish; i.e., the terms that are related to  $a_{6,8}$  disappear from the decay amplitudes for case II. As to the parameters  $H(BM_1, M_2)$  and  $H'(BM_1, M_2)$  in  $a_{i,II}$ , they are defined as

$$\begin{aligned}
H(BP, V) &= \frac{f_B f_P}{m_B^2 F_1^{B \rightarrow P}(0)} \int_0^1 d\xi \int_0^1 dx \int_0^1 dy \frac{\Phi_B(\xi)}{\xi} \\
&\quad \times \frac{\Phi_V(x)}{\bar{x}} \left[ \frac{\Phi_P(y)}{\bar{y}} + \frac{2\mu_P \bar{x}}{m_b} \frac{\Phi_P^p(y)}{\bar{y}} \right], \\
H'(BP, V) &= -\frac{f_B f_P}{m_B^2 F_1^{B \rightarrow P}(0)} \int_0^1 d\xi \int_0^1 dx \int_0^1 dy \frac{\Phi_B(\xi)}{\xi} \\
&\quad \times \frac{\Phi_V(x)}{x} \left[ \frac{\Phi_P(y)}{\bar{y}} + \frac{2\mu_P x}{m_b} \frac{\Phi_P^p(y)}{\bar{y}} \right]. \tag{14}
\end{aligned}$$

The parameter  $\mu_P = m_P^2/(m_1 + m_2)$ , where  $m_{1,2}$  are the current quark masses of the meson constituents, is proportional to the chiral quark condensate.

## B. Annihilation parameters $b_i$

The parameters of  $b_i$  in Eq. (5) correspond to weak-annihilation contributions. Now we give their expressions, which are analogous to those in [23]:

$$b_1(M_1, M_2) = \frac{C_F}{N_c^2} C_1 A_1^i(M_1, M_2),$$

$$b_2(M_1, M_2) = \frac{C_F}{N_c^2} C_2 A_1^i(M_1, M_2),$$

$$\begin{aligned}
b_3(M_1, M_2) &= \frac{C_F}{N_c^2} \{ C_3 A_1^i(M_1, M_2) + C_5 A_3^i(M_1, M_2) \\
&\quad + [C_5 + N_c C_6] A_3^f(M_1, M_2) \},
\end{aligned}$$

$$b_4(M_1, M_2) = \frac{C_F}{N_c^2} \{ C_4 A_1^i(M_1, M_2) + C_6 A_2^i(M_1, M_2) \},$$

$$b_3^{ew}(M_1, M_2) = \frac{C_F}{N_c^2} \{C_9 A_1^i(M_1, M_2) + C_7 A_3^i(M_1, M_2) \\ + [C_7 + N_c C_8] A_3^f(M_1, M_2)\},$$

$$b_4^{ew}(M_1, M_2) = \frac{C_F}{N_c^2} \{C_{10} A_1^i(M_1, M_2) + C_8 A_2^i(M_1, M_2)\}. \quad (15)$$

Here the current-current annihilation parameters  $b_{1,2}(M_1, M_2)$  arise from the hadronic matrix elements of the effective operators  $\mathcal{O}_{1,2}$ , the QCD penguin annihilation parameters  $b_{3,4}(M_1, M_2)$  from  $\mathcal{O}_{3-6}$ , and the electroweak penguin annihilation parameters  $b_{3,4}^{ew}(M_1, M_2)$  from  $\mathcal{O}_{7-10}$ . The parameters of  $b_i$  are closely related to the final states; they can also be divided into two different cases according to the final states. Case I is that  $M_1$  is a vector meson and  $M_2$  is a pseudoscalar meson (here  $M_1$  and  $M_2$  are tagged in Fig. 3). Case II is that  $M_1$  corresponds to a pseudoscalar meson and  $M_2$  corresponds to a vector meson. For case I, the definitions of  $A_k^{i,f}(M_1, M_2)$  in Eq. (15) are

$$A_{1,2}^f(V, P) = 0,$$

$$A_3^f(V, P) = \pi \alpha_s \int_0^1 dx \int_0^1 dy \Phi_V(x) \Phi_P^p(y) \frac{2\mu_P}{m_b} \frac{2(1+\bar{x})}{\bar{x}^2 y},$$

$$A_1^i(V, P) = \pi \alpha_s \int_0^1 dx \int_0^1 dy \Phi_V(x) \Phi_P(y) \\ \times \left[ \frac{1}{y(1-x\bar{y})} + \frac{1}{\bar{x}^2 y} \right],$$

$$A_2^i(V, P) = -\pi \alpha_s \int_0^1 dx \int_0^1 dy \Phi_V(x) \Phi_P(y) \\ \times \left[ \frac{1}{\bar{x}(1-x\bar{y})} + \frac{1}{\bar{x} y^2} \right],$$

$$A_3^i(V, P) = \pi \alpha_s \int_0^1 dx \int_0^1 dy \Phi_V(x) \Phi_P^p(y) \\ \times \frac{2\mu_P}{m_b} \frac{2\bar{y}}{\bar{x} y(1-x\bar{y})}. \quad (16)$$

For case II,

$$A_{1,2}^f(P, V) = 0,$$

$$A_3^f(P, V) = -\pi \alpha_s \int_0^1 dx \int_0^1 dy \Phi_P^p(x) \Phi_V(y) \\ \times \frac{2\mu_P}{m_b} \frac{2(1+y)}{\bar{x} y^2},$$

$$A_1^i(P, V) = \pi \alpha_s \int_0^1 dx \int_0^1 dy \Phi_P(x) \Phi_V(y) \\ \times \left[ \frac{1}{y(1-x\bar{y})} + \frac{1}{\bar{x}^2 y} \right],$$

$$A_2^i(P, V) = -\pi \alpha_s \int_0^1 dx \int_0^1 dy \Phi_P(x) \Phi_V(y) \\ \times \left[ \frac{1}{\bar{x}(1-x\bar{y})} + \frac{1}{\bar{x} y^2} \right],$$

TABLE II. Experimentally known data of  $CP$ -averaged branching ratios for the charmless  $B \rightarrow PV$  decay modes, used as input for the global fit. The channels containing the  $\eta'$  meson have been excluded.

$BR (\times 10^6)$	BaBar [1–10]	Belle [11–15]	CLEO [16–21]	Average
$B^0 \rightarrow \pi^\pm \rho^\mp$	$28.9 \pm 5.4 \pm 4.3$	$20.8^{+6.0+2.8}_{-6.3-3.1}$	$27.6^{+8.4}_{-7.4} \pm 4.2$	$25.53 \pm 4.32$
$B^+ \rightarrow \pi^+ \rho^0$	$24 \pm 8 \pm 3 (< 39)$	$8.0^{+2.3}_{-2.0} \pm 0.7$	$10.4^{+3.3}_{-3.4} \pm 2.1$	$9.49 \pm 2.57$
$B^0 \rightarrow \pi^0 \rho^0$	$3.6 \pm 3.5 \pm 1.7 (< 10.6)$	$< 5.3$	$1.6^{+2.0}_{-1.4} \pm 0.8 (< 5.5)$	$2.07 \pm 1.88$
$B^+ \rightarrow \pi^+ \omega$	$6.6^{+2.1}_{-1.8} \pm 0.7$	$4.2^{+2.0}_{-1.8} \pm 0.5$	$11.3^{+3.3}_{-2.9} \pm 1.4$	$6.22 \pm 1.70$
$B^0 \rightarrow K^+ \rho^-$	–	$15.8^{+5.1}_{-4.6-3.0}$	$16.0^{+7.6}_{-6.4} \pm 2.8 (< 32)$	$15.88 \pm 4.65$
$B^+ \rightarrow K^+ \rho^0$	$10 \pm 6 \pm 2 (< 29)$	–	$8.4^{+4.0}_{-3.4} \pm 1.8 (< 17)$	$8.92 \pm 3.60$
$B^+ \rightarrow K^+ \omega$	$1.4^{+1.3}_{-1.0} \pm 0.3 (< 4)$	$9.2^{+2.6}_{-2.3} \pm 1.0$	$3.2^{+2.4}_{-1.9} \pm 0.8 (< 7.9)$	$2.92 \pm 1.94$
$B^0 \rightarrow K^0 \omega$	$5.9^{+1.7}_{-1.5} \pm 0.9$	–	$10.0^{+5.4}_{-4.2} \pm 1.4 (< 21)$	$6.34 \pm 1.82$
$B^0 \rightarrow K^{*+} \pi^-$	–	$26.0 \pm 8.3 \pm 3.5$	$16^{+6}_{-5} \pm 2$	$19.3 \pm 5.2$
$B^+ \rightarrow K^{*0} \pi^-$	$15.5 \pm 3.4 \pm 1.8$	$19.4^{+4.2}_{-3.9} \pm 2.1^{+3.5}_{-6.8}$	$7.6^{+3.5}_{-3.0} \pm 1.6 (< 16)$	$12.12 \pm 3.13$
$B^+ \rightarrow K^{*-} \pi^0$	–	–	$7.1^{+11.4}_{-7.1} \pm 1.0 (< 31)$	$7.1 \pm 11.4$
$B^+ \rightarrow K^{*+} \eta$	$22.1^{+11.1}_{-9.2} \pm 3.3$	$26.5^{+7.8}_{-7.0} \pm 3.0$	$26.4^{+9.6}_{-8.2} \pm 3.3$	$25.4 \pm 5.6$
$B^0 \rightarrow K^{*0} \eta$	$19.8^{+6.5}_{-5.6} \pm 1.7$	$16.5^{+4.6}_{-4.2} \pm 1.2$	$13.8^{+5.5}_{-4.6} \pm 1.6$	$16.41 \pm 3.21$
$B^+ \rightarrow K^+ \phi$	$9.2 \pm 1.0 \pm 0.8$	$10.7 \pm 1.0^{+0.9}_{-1.6}$	$5.5^{+2.1}_{-1.8} \pm 0.6$	$8.58 \pm 1.24$
$B^0 \rightarrow K^0 \phi$	$8.7^{+1.7}_{-1.5} \pm 0.9$	$10.0^{+1.9}_{-1.7-1.3} \pm 0.9$	$5.4^{+3.7}_{-2.7} \pm 0.7 (< 12.3)$	$8.72 \pm 1.37$

TABLE III. Experimental measured data of direct  $CP$  asymmetries for the charmless  $B \rightarrow PV$  decay modes, used as input for the global fit.

$\mathcal{A}_{CP}$	BaBar [1–10]	Belle [11–15]	CLEO [16–21]	Average
$B^- \rightarrow \pi^- \omega$	$-0.01^{+0.29}_{-0.31} \pm 0.03$	–	$-0.34 \pm 0.25 \pm 0.02$	$-0.21 \pm 0.19$
$B^- \rightarrow K^- \omega$	–	$-0.21 \pm 0.28 \pm 0.03$	–	$-0.21 \pm 0.28$
$B^- \rightarrow K^{*-} \eta$	–	$-0.05^{+0.25}_{-0.30} \pm 0.01$	–	$-0.05 \pm 0.30$
$\bar{B}^0 \rightarrow \bar{K}^{*0} \eta$	–	$0.17^{+0.28}_{-0.25} \pm 0.01$	–	$0.17 \pm 0.28$
$B^- \rightarrow K^- \phi$	$-0.05 \pm 0.20 \pm 0.03$	–	–	$-0.05 \pm 0.20$

$$A_3^i(P, V) = \pi \alpha_s \int_0^1 dx \int_0^1 dy \Phi_P^i(x) \Phi_V(y) \times \frac{2\mu_P}{m_b} \frac{2x}{\bar{x}y(1-xy)}. \quad (17)$$

Here our notation and convention are the same as those in [23]. The superscripts  $i$  and  $f$  on  $A^{i,f}$  correspond to the contributions from Figs. 3(a),(b) and 3(c),(d), respectively. The subscripts  $k=1, 2$ , and  $3$  on  $A_k^{i,f}$  refer to the Dirac structures  $(V-A) \otimes (V-A)$ ,  $(V-A) \otimes (V+A)$ , and  $(-2)(S-P) \otimes (S+P)$ , respectively.  $\Phi_V(x)$  denotes the leading-twist LCDAs of a vector meson, and  $\Phi_P(x)$  and  $\Phi_P^i(x)$  denote twist-2 and twist-3 LCDAs of a pseudoscalar meson, respectively.

Note that assuming SU(3) flavor symmetry implies symmetric LCDAs of light mesons (under  $x \leftrightarrow \bar{x}$ ), whence  $A_1^i = -A_2^i$ . In this approximation the weak-annihilation contributions (for case I) can be parametrized as

$$\begin{aligned} A_1^i(V, P) &\approx 18\pi\alpha_s \left( X_A - 4 + \frac{\pi^2}{3} \right), \\ A_3^i(V, P) &\approx \pi\alpha_s r_\chi [2\pi^2 - 6(X_A^2 + 2X_A)], \\ A_3^f(V, P) &\approx 6\pi\alpha_s r_\chi (2X_A^2 - X_A), \end{aligned} \quad (18)$$

where  $X_A = \int_0^1 dx/x$  parametrizes the divergent end-point integrals and  $r_\chi = 2\mu_P/m_b$  is the so-called *chirally enhanced* factor. We can get similar forms to Eq. (18) for case II, but with  $A_3^f(P, V) = -A_3^f(V, P)$ . In our calculation, we will treat  $X_A$  as a phenomenological parameter and take the same value for all annihilation terms, although this approximation

TABLE IV. Experimental results and correlation matrix for the various asymmetries measured in the channels  $\rho^\pm \pi^\mp / \rho^\pm K^\mp$ . The notation is explained in [9].

$B^0 \rightarrow \rho^\pm \pi^\mp$	Measurement	Correlation coefficient (%)			
		$\mathcal{A}_{CP}^{\rho\pi}$	$\mathcal{A}_{CP}^{\rho K}$	$C_{\rho\pi}$	$\Delta C_{\rho\pi}$
$\mathcal{A}_{CP}^{\rho\pi}$	$-0.22 \pm 0.08 \pm 0.07$	–	3.4	-11.8	-10.4
$\mathcal{A}_{CP}^{\rho K}$	$0.19 \pm 0.14 \pm 0.11$	3.4	–	-1.3	-1.1
$C_{\rho\pi}$	$0.45^{+0.18}_{-0.19} \pm 0.09$	-11.8	-1.3	–	23.9
$\Delta C_{\rho\pi}$	$0.38^{+0.19}_{-0.20} \pm 0.11$	-10.4	-1.1	23.9	–

is crude and there is no known physical argument justifying this assumption. We shall see below that  $X_A$  gives large uncertainties in the theoretical prediction.

#### IV. QCD FACTORIZATION VERSUS EXPERIMENT

In order to propose a test of QCD factorization with respect to experiment, a compilation of various charmless branching fractions and direct  $CP$  asymmetries was performed and is given in Tables II, III, and IV. This compilation includes the latest results from BaBar, Belle, and CLEO. The measurements were combined into a single central value and error, which may be compared with the theoretical prediction. First, the total error from each experiment was computed by summing quadratically the statistic and systematic error: this approach is valid in the limit that the systematic error is not so large with respect to the statistic error. Second, when the experiment provides an asymmetric error  $^{+\sigma_1}_{-\sigma_2}$ , a conservative symmetric error was assumed in the calculation by using  $\pm \text{Max}(\sigma_1, \sigma_2)$ . In case of a disagreement between several experiments for a given measurement, the total error was increased by a “scale factor” computed from a  $\chi^2$  combining the various experiments, using the standard procedure given by the Particle Data Group (PDG) [43].

In order to compare the theoretical predictions  $\{y\}$  with the experimental measurements  $\{x \pm \sigma_x\}$ , the following  $\chi^2$  was defined:

$$\chi^2 = \sum \left( \frac{x-y}{\sigma_x} \right)^2.$$

In the case when a correlation matrix between several measurements is given by the experiment, as in the case of the  $\rho^+ \pi^- / \rho^+ K^-$  measurements, the  $\chi^2$  was corrected to account for it. The above  $\chi^2$  was then minimized using MINUIT [44], letting free all theoretical parameters in their allowed range. The quality of the minimum yielded by MINUIT was assessed by replacing it with an *ad hoc* minimizer scanning the entire parameter space. The theoretical predictions, with the theoretical parameters yielding the best fits, are compared to experiment in Table V for two scenarios to be explained below. The asymmetries of the  $\rho^\pm \pi^\mp$  channels can be expressed [9] in terms of the quantities reported in Table IV. The comparison between their theoretical predictions and experiment is reported in Table VI.

Scenario 1 refers to a fit according to QCD factorization, varying all theoretical parameters in the range presented in

TABLE V. Best-fit values using the global analysis of  $B \rightarrow PV$  decays in QCDF with free  $\gamma$  (scenario 1) and QCDF+charming penguin diagrams (scenario 2) with constrained  $\gamma$ . The  $CP$ -averaged branching ratios are in units of  $10^{-6}$ .

	Experiment	Scenario 1		Scenario 2	
		Prediction	$\chi^2$	Prediction	$\chi^2$
$\mathcal{BR}(\bar{B}^0 \rightarrow \rho^0 \pi^0)$	$2.07 \pm 1.88$	0.132	1.1	0.177	1.0
$\mathcal{BR}(\bar{B}^0 \rightarrow \rho^+ \pi^-)$		11.023		10.962	
$\mathcal{BR}(\bar{B}^0 \rightarrow \rho^- \pi^+)$		18.374		17.429	
$\mathcal{BR}(\bar{B}^0 \rightarrow \rho^\pm \pi^\mp)$	$25.53 \pm 4.32$	29.397	0.8	28.391	0.4
$\mathcal{BR}(B^- \rightarrow \rho^0 \pi^-)$	$9.49 \pm 2.57$	9.889	0.0	7.879	0.4
$\mathcal{BR}(B^- \rightarrow \omega \pi^-)$	$6.22 \pm 1.7$	6.002	0.0	5.186	0.4
$\mathcal{BR}(B^- \rightarrow K^{*0} K^-)$		0.457		0.788	
$\mathcal{BR}(B^- \rightarrow K^{*0} K^-)$		0.490		0.494	
$\mathcal{BR}(B^- \rightarrow \Phi \pi^-)$		0.004		0.003	
$\mathcal{BR}(B^- \rightarrow \rho^- \pi^0)$		9.646		11.404	
$\mathcal{BR}(\bar{B}^0 \rightarrow \rho^0 \bar{K}^0)$		5.865		8.893	
$\mathcal{BR}(\bar{B}^0 \rightarrow \omega \bar{K}^0)$	$6.34 \pm 1.82$	2.318	4.9	5.606	0.2
$\mathcal{BR}(\bar{B}^0 \rightarrow \rho^+ K^-)$	$15.88 \pm 4.65$	6.531	4.0	14.304	0.1
$\mathcal{BR}(\bar{B}^0 \rightarrow K^{*0} \pi^+)$	$19.3 \pm 5.2$	9.760	3.4	10.787	2.7
$\mathcal{BR}(B^- \rightarrow K^{*0} \pi^0)$	$7.1 \pm 11.4$	7.303	0.0	8.292	0.0
$\mathcal{BR}(\bar{B}^0 \rightarrow \Phi \bar{K}^0)$	$8.72 \pm 1.37$	8.360	0.1	8.898	0.0
$\mathcal{BR}(B^- \rightarrow \bar{K}^{*0} \pi^-)$	$12.12 \pm 3.13$	7.889	1.8	11.080	0.1
$\mathcal{BR}(B^- \rightarrow \rho^0 K^-)$	$8.92 \pm 3.6$	1.882	3.8	5.655	0.8
$\mathcal{BR}(B^- \rightarrow \rho^- \bar{K}^0)$		7.140		14.006	
$\mathcal{BR}(B^- \rightarrow \omega K^-)$	$2.92 \pm 1.94$	2.398	0.1	6.320	3.1
$\mathcal{BR}(B^- \rightarrow \Phi K^-)$	$8.88 \pm 1.24$	8.941	0.0	9.479	0.2
$\mathcal{BR}(\bar{B}^0 \rightarrow \bar{K}^{*0} \eta)$	$16.41 \pm 3.21$	22.807	4.0	18.968	0.6
$\mathcal{BR}(B^- \rightarrow K^{*0} \eta)$	$25.4 \pm 5.6$	17.855	1.8	15.543	3.1
$\Delta C_{\rho\pi}$	$0.38 \pm 0.23$	0.250	} 8.1/4	0.228	} 3.9/4
$C_{\rho\pi}$	$0.45 \pm 0.21$	0.019		0.092	
$\mathcal{A}_{CP}^{\rho\pi}$	$-0.22 \pm 0.11$	-0.015		-0.115	
$\mathcal{A}_{CP}^{\rho K}$	$0.19 \pm 0.18$	0.060		0.197	
$\mathcal{A}_{CP}^{\omega\pi^-}$	$-0.21 \pm 0.19$	-0.072	0.5	-0.198	0.0
$\mathcal{A}_{CP}^{\omega K^-}$	$-0.21 \pm 0.28$	0.029	0.7	0.189	2.0
$\mathcal{A}_{CP}^{\eta K^{*0}}$	$-0.05 \pm 0.3$	-0.138	0.1	-0.217	0.3
$\mathcal{A}_{CP}^{\eta \bar{K}^{*0}}$	$0.17 \pm 0.28$	-0.186	1.6	-0.158	1.4
$\mathcal{A}_{CP}^{\phi K^-}$	$-0.05 \pm 0.2$	0.006	0.1	0.005	0.1
			36.9		20.8

Table VII. Even the unitarity triangle angle  $\gamma$  is varied freely and ends up not far from  $90^\circ$ . We have taken  $X_A = X_H$  in the range proposed in Ref. [23]:

$$X_{A,H} = \int_0^1 \frac{dx}{x} = \ln \frac{m_B}{\Lambda_h} (1 + \rho_{A,H} e^{i\phi_{A,H}}). \quad (19)$$

TABLE VI. Values of the  $CP$  asymmetries for  $B \rightarrow \pi\rho$  decays in QCDF (scenario 1) and QCDF+charming penguin diagrams (scenario 2). The notation is explained in [9].

	Experiment	Scenario 1	Scenario 2
$\mathcal{A}_{CP}^{\rho^+ \pi^-}$	$-0.82 \pm 0.31 \pm 0.16$	-0.04	-0.23
$\mathcal{A}_{CP}^{\rho^- \pi^+}$	$-0.11 \pm 0.16 \pm 0.09$	-0.0002	0.04

These parameters label our ignorance of the nonperturbatively calculable subdominant contribution to the annihilation and hard scattering, defined in Eqs. (16),(17) and Eqs. (13),(14), respectively. They do not need to have the same value for all  $PV$  channels but we have nevertheless assumed one common value since a fit would become impossible with too many unknown parameters.

Scenario 2 in Table V refers to a fit adding a charming-penguin-diagram-inspired long-distance contribution which

TABLE VII. Various theoretical inputs used in our global analysis of  $B \rightarrow PV$  decays in QCDF. The parameter ranges have been taken from literature [23,34,35,45]. The two last columns give the best fits of both scenarios.

Input	Range	Scenario 1	Scenario 2
$\gamma$ (deg)		99.955	81.933
$m_s$ (GeV)	[0.085,0.135]	0.085	0.085
$\mu$ (GeV)	[2.1,8.4]	3.355	5.971
$\rho_A$	[-1,1]	1.000	1.000
$\phi_A$ (deg)	[-180,180]	-22.928	-87.907
$\lambda_B$ (GeV)	[0.2,0.5]	0.500	0.500
$f_B$ (GeV)	[0.14,0.22]	0.220	0.203
$R_u$	[0.35,0.49]	0.350	0.350
$R_c$	[0.018,0.025]	0.018	0.018
$A_0^{B \rightarrow \rho}$	[0.3162,0.4278]	0.373	0.377
$F_1^{B \rightarrow \pi}$	[0.23,0.33]	0.330	0.301
$A_0^{B \rightarrow \omega}$	[0.25,0.35]	0.350	0.326
$A_0^{B \rightarrow K^*}$	[0.3995,0.5405]	0.400	0.469
$F_1^{B \rightarrow K}$	[0.28,0.4]	0.333	0.280
$\text{Re}[\mathcal{A}^P]$	[-0.01,0.01]		0.00253
$\text{Im}[\mathcal{A}^P]$	[-0.01,0.01]		-0.00181
$\text{Re}[\mathcal{A}^V]$	[-0.01,0.01]		-0.00187
$\text{Im}[\mathcal{A}^V]$	[-0.01,0.01]		0.00049

will be presented and discussed in Sec. V. In this fit  $\gamma$  is constrained within the range  $[34^\circ, 82^\circ]$ .

The values of the theoretical parameters found for the two best fits is given in Table VII: many parameters are found to be at the edge of their allowed range.<sup>1</sup> In order to estimate the quality of the agreement between measurements and predictions, the standard Monte Carlo based “goodness of fit” test was performed.

(i) The best-fit values of the theoretical parameters were used to make predictions for the branching ratios and  $CP$  asymmetries.

(ii) The total experimental error from each measurement was used to generate new experimental values distributed around the predictions with a Gaussian probability.

(iii) The full fit previously performed on real measurements is now run on this simulated data, and the  $\chi^2$  of this fit is saved in a histogram  $H$ .

It is then possible to compare the  $\chi_{\text{data}}^2$  obtained from the measurement with the  $\chi^2$  one would obtain if the predictions were true. Additionally, one may compute the confidence level of the tested model by using

$$\text{C.L.} \leq \frac{\int_{\chi^2 > \chi_{\text{data}}^2} H(\chi^2) d\chi^2}{\int_{\chi^2 > 0} H(\chi^2) d\chi^2}.$$

The results of the “goodness of fit” tests are given in Fig. 4. From these tests, one may quote an upper limit for the confidence level in scenario 1,  $\text{C.L.} \leq 0.1\%$  and, in the case of scenario 2,  $\text{C.L.} \leq 7.7\%$ .

In Tables II (III) we give the experimental  $CP$ -averaged branching ratios (direct  $CP$  asymmetries) which we have used in our fits. We have also used the quantities reported in Table IV which are related to the branching ratios and  $CP$  asymmetries of the  $B \rightarrow \rho^\pm \pi^\mp$  channels.

For the sake of definiteness let us recall that the branching ratios for any charmless  $B$  decays,  $B \rightarrow PV$  channel, in the rest frame of the  $B$  meson, is given by

$$\begin{aligned} \mathcal{BR}(B \rightarrow PV) = \frac{\tau_B}{8\pi} \frac{|p|}{m_B^2} & |\mathcal{A}(B \rightarrow PV) + \mathcal{A}^a(B \rightarrow PV) \\ & + \mathcal{A}^{\text{LD}}(B \rightarrow PV)|^2, \end{aligned} \quad (20)$$

where  $\tau_B$  represents the  $B$ -meson lifetime (charged or uncharged according to the case). The amplitudes  $\mathcal{A}, \mathcal{A}^a$  and  $\mathcal{A}^{\text{LD}}$  are defined in Appendixes A, B and in Eqs. (24) and (25), respectively. In the case of pure QCD factorization (scenario 1) we take of course  $\mathcal{A}^{\text{LD}}=0$ . The kinematical factor  $|p|$  is written as

$$|p| = \frac{\sqrt{[m_B^2 - (m_P + m_V)^2][m_B^2 - (m_P - m_V)^2]}}{2m_B}. \quad (21)$$

### Comparison with Du *et al.*

Our negative conclusion about the QCD factorization fit of the  $B \rightarrow PV$  channels is at odds with the conclusion of the authors of Ref. [36], who have performed a successful fit of both  $B \rightarrow PP$  and  $B \rightarrow PV$  channels using the same theoretical starting point. These authors have excluded from their fits the channels containing a  $K^*$  in the final state, arguing that these channels seemed questionable to them. We have thus made a fit without the channels containing the  $K^*$ , and indeed we find as the authors of Ref. [36] that the global agreement between QCD factorization and experiment was satisfactory. Notice that this fit was done without discarding the channels  $B^+ \rightarrow \omega \pi^+(K^+)$  as done by Du *et al.*

Notice also that the parameters  $C_{\rho\pi}$  and the  $A_{CP}^{\rho\pi}$  have been kept in this fit. The disagreement between QCDF and experiment for these quantities was not enough to spoil the satisfactory agreement of the global fit because the experimental errors are still large on these quantities.

The conclusion of this subsection is that the difference between the “optimistic” conclusion about QCDF of Du *et al.* and our rather pessimistic one comes from their choice of discarding the channels containing the  $K^*$ 's. In other words the conclusion about the status of QCDF in the  $B \rightarrow PV$  channels depends on the confidence we give to the

<sup>1</sup>Table VII shows that the fit value of  $\rho_A$  appears at the edge of the input range,  $\rho_A=1$ . However enlarging the range of  $\rho_A$ , such as  $|\rho_A| \leq 10$ , brings a large annihilation contribution  $(\rho_A, \phi_A) = (2.3, -41^\circ)$  for scenario 1 and  $(4.4, -108^\circ)$  for scenario 2. With so large values of  $|\rho_A|$  the unpredictable contributions would dominate the total result making the whole exercise void of signification.

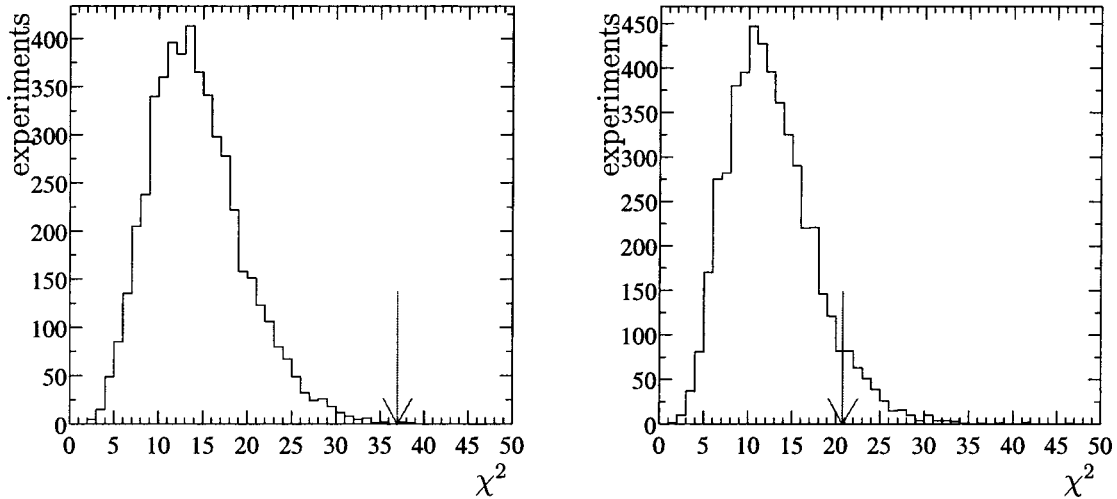


FIG. 4. Goodness-of-fit test of the two proposed theoretical models: the arrow points at the value  $\chi_{\text{data}}^2$  found from the measurements, and the histogram shows the values allowed for  $\chi^2$  in the case that the models predictions are correct.

published results on these channels.

### V. SIMPLE MODEL FOR LONG-DISTANCE INTERACTIONS

As seen in Table V the failure of our overall fit with QCDF can be traced to two main facts. First the strange branching ratios are underestimated by QCDF. Second the direct  $CP$  asymmetries in the nonstrange channels might also be underestimated. *A priori* this could be cured if some nonperturbative mechanism were contributing to  $|P|$ . Indeed, first, in the strange channels,  $|P|$  is Cabibbo enhanced and such a nonperturbative contribution could increase the branching ratios, and second, increasing  $|P|/|T|$  in the nonstrange channels with nonsmall strong phases could increase significantly the direct  $CP$  asymmetries as already discussed. We have therefore tried a charming-penguin-diagram-inspired model. We wanted nevertheless to avoid to add too many new parameters which would make the fit void of significance. We have therefore tried a model for long-distance penguin contributions which depends only on two fitted complex numbers.

Let us start by describing our charming-penguin-diagram-inspired model for strange final states. In the “charming penguin diagram” picture the weak decay of a  $\bar{B}^0$  ( $B^-$ ) meson through the action of the operator  $Q_1^c$  [see notation in Eqs. (1) and (2)] creates an hadronic system containing the quarks  $s, \bar{d}(\bar{u}), c, \bar{c}$ , for example  $\bar{D}_s^{(*)} + D^{(*)}$  systems. This system goes to long distances, the  $c, \bar{c}$  eventually annihilate, a pair of light quarks are created by a nonperturbative strong interaction and one is left with two light mesons. Let us here restrict ourselves to the case of a  $PV$  pair of mesons; i.e., one of the final mesons is a light pseudoscalar ( $\pi, K, \eta$ ) and the other a light vector meson ( $\rho, \omega, \phi, K^*$ ). In this paper we leave aside the  $\eta'$  which is presumably quite special.

We will picture now this hadronic system as a coherent state which decays into the two final mesons with total strangeness  $-1$ . This state has a total angular momentum  $J=0$ . Its flavor  $s\bar{d}$  is that of a member of an octet of flavor-

SU(3) symmetry. We will assume flavor-SU(3) symmetry in the decay amplitude of this hadronic state. This still leaves four SU(3)-invariant amplitudes since both  $P$  and  $V$  can have an octet and a singlet component and that there exist two octets in the decomposition of  $8 \times 8$ . We make a further simplifying assumption based on the Okubo-Zweig-Iizuka (OZI) rule. Let us give an example: we assume that  $V=(s\bar{q})$  where  $q$  is any of the light quarks  $u, d, s$ , and that  $P=(q\bar{d})$ . Then we compute the contractions between

$$\langle (s\bar{q})(q\bar{d}) | s(\bar{u}u + \bar{d}d + \bar{s}s)\bar{d} \rangle = 1. \quad (22)$$

The meaning of this rule is simple. We add to the  $s\bar{d}$  quarks in our hadronic state an SU(3) singlet  $\bar{u}u + \bar{d}d + \bar{s}s$  and compute an “overlap” making contractions so that the quarks in the singlet go into two different mesons. This latter constraint is the OZI rule. This is why the overlap in Eq. (22) is 1 even if  $q=d$  since it is forbidden to have both  $d$  quarks from the singlet in the same final meson. As an example, the decay  $B \rightarrow \bar{K}^0 \rho^0$  gives the following overlap coefficient:

$$\left\langle (s\bar{d}) \frac{(u\bar{u} - d\bar{d})}{\sqrt{2}} \middle| s(\bar{u}u + \bar{d}d + \bar{s}s)\bar{d} \right\rangle = -\frac{1}{\sqrt{2}}. \quad (23)$$

For the  $\eta$  meson we will use the decomposition in [32]. The overlap coefficients thus computed play the role of SU(3) Clebsch-Gordan (CG) coefficients computed in a simple way. These coefficients are assumed to be multiplied by an universal complex amplitude to be fitted from experiment. Up to now we have assumed that the active quark (here,  $s$ ) ended up in the vector meson. We need another universal amplitude for the case where the active quark ends up in the pseudoscalar meson.

We are thus left with two theoretically independent and unknown amplitudes: one with  $V=(s\bar{q})$ ,  $P=(q\bar{d})$ , one with  $P=(s\bar{q})$ ,  $V=(q\bar{d})$ . We shall write them respectively as  $\mathcal{A}^P$  ( $\mathcal{A}^V$ ) when the active quark ends up in the pseudoscalar (vector) meson.

TABLE VIII. Flavor-SU(3) Clebsch-Gordan coefficient for long-distance penguin-diagram-like contributions. Notice that the channel  $B^- \rightarrow \Phi \pi^-$  vanishes due to the OZI rule.

	$Cl^P$	$Cl^V$
$\mathcal{BR}(\bar{B}^0 \rightarrow \rho^0 \pi^0)$	0.5	0.5
$\mathcal{BR}(\bar{B}^0 \rightarrow \rho^+ \pi^-)$	1.0	0.
$\mathcal{BR}(\bar{B}^0 \rightarrow \rho^- \pi^+)$	0.	1.0
$\mathcal{BR}(B^- \rightarrow \rho^0 \pi^-)$	$1/\sqrt{2}$	$-1/\sqrt{2}$
$\mathcal{BR}(B^- \rightarrow \omega \pi^-)$	$1/\sqrt{2}$	$1/\sqrt{2}$
$\mathcal{BR}(B^- \rightarrow K^{*0} K^0)$	1.0	0.
$\mathcal{BR}(B^- \rightarrow K^{*0} K^-)$	0.	1.0
$\mathcal{BR}(B^- \rightarrow \Phi \pi^-)$	0.	0.
$\mathcal{BR}(B^- \rightarrow \rho^- \pi^0)$	$-1/\sqrt{2}$	$1/\sqrt{2}$
$\mathcal{BR}(\bar{B}^0 \rightarrow \rho^0 \bar{K}^0)$	$-1/\sqrt{2}$	0.
$\mathcal{BR}(\bar{B}^0 \rightarrow \omega \bar{K}^0)$	$1/\sqrt{2}$	0.
$\mathcal{BR}(\bar{B}^0 \rightarrow \rho^+ K^-)$	1.0	0.
$\mathcal{BR}(\bar{B}^0 \rightarrow K^{*-} \pi^+)$	0.	1.0
$\mathcal{BR}(B^- \rightarrow K^{*-} \pi^0)$	0.	$1/\sqrt{2}$
$\mathcal{BR}(\bar{B}^0 \rightarrow \Phi \bar{K}^0)$	0.	1.0
$\mathcal{BR}(B^- \rightarrow \bar{K}^{*0} \pi^-)$	0.	1.0
$\mathcal{BR}(B^- \rightarrow \rho^0 K^-)$	$1/\sqrt{2}$	0.
$\mathcal{BR}(B^- \rightarrow \rho^- \bar{K}^0)$	1.0	0.
$\mathcal{BR}(B^- \rightarrow \omega K^-)$	$1/\sqrt{2}$	0.
$\mathcal{BR}(B^- \rightarrow \Phi K^-)$	0.	1.0
$\mathcal{BR}(\bar{B}^0 \rightarrow \bar{K}^{*0} \eta)$	-0.665	0.469
$\mathcal{BR}(B^- \rightarrow K^{*-} \eta)$	-0.665	0.469

Concerning the  $\bar{B}$  decay into a pseudoscalar + vector meson of vanishing total strangeness, we apply the same recipe with the same amplitudes  $\mathcal{A}^P$  and  $\mathcal{A}^V$ , replacing the  $s$  quark by a  $d$  quark and, of course, the corresponding replacement of the CKM factor  $V_{cb}V_{cs}^*$  by  $V_{cb}V_{cd}^*$ .

To summarize, the long-distance term is given by two universal complex amplitudes multiplied by a CG coefficient computed simply by the overlap factor in Eq. (23); see Table VIII.

In practice, to the amplitudes described in the Appendixes we add the long-distance amplitudes, given by

$$\mathcal{A}^{\text{LD}}(B \rightarrow PV) = \frac{G_F}{\sqrt{2}} m_B^2 \lambda_c' (Cl^P \mathcal{A}^P + Cl^V \mathcal{A}^V) \quad (24)$$

for the nonstrange channels and

$$\mathcal{A}^{\text{LD}}(B \rightarrow PV) = \frac{G_F}{\sqrt{2}} m_B^2 \lambda_c (Cl^P \mathcal{A}^P + Cl^V \mathcal{A}^V) \quad (25)$$

for the strange channels. In Eqs. (24) and (25),  $\mathcal{A}^P$  and  $\mathcal{A}^V$  are two complex numbers which are fitted in the global fit of scenario 2 and  $Cl^P$  and  $Cl^V$  are the flavor-SU(3) Clebsch-Gordan coefficients which are given in Table VIII. For both channels containing the  $\eta$  we have used the formulas

$$Cl^V = \frac{\cos \theta_8}{\sqrt{6}} - \frac{\sin \theta_0}{\sqrt{3}}, \quad Cl^P = -2 \frac{\cos \theta_8}{\sqrt{6}} - \frac{\sin \theta_0}{\sqrt{3}}, \quad (26)$$

with  $\theta_0 = -9.1^\circ$  and  $\theta_8 = -22.2^\circ$ .

The fit with long-distance penguin contributions is presented in Table V under the label ‘‘Scenario 2.’’ The agreement with experiment is improved, and it should be so, but not in such a fully convincing manner. The goodness of the fit is about 8% which implies that this model is not excluded by experiment. However, a look at Table VII shows that several fitted parameters are still stuck at the end of the allowed range of variation. In particular  $\rho_A = 1$  means that the uncalculable subleading contribution to QCDF is again stretched to its extreme.

Finally the fitted complex numbers which fix the size of the long-distance penguin contribution (last four lines in Table VII) are small. To make this statement quantitative, assuming the long-distance amplitude were alone, the values for  $\mathcal{A}^P$  and  $\mathcal{A}^V$  in Table V correspond to branching ratios which reach at their maximum  $6 \times 10^{-6}$  but are more generally in the vicinity of  $2 \times 10^{-6}$ . In part, this is due to the fact that, if some strange channels want a large nonperturbative contribution to increase their branching ratios, some other strange channels and particularly the  $B \rightarrow K\phi$  channels which are in good agreement with QCDF cannot accept the addition of a too large nonperturbative penguin contribution. This last point should be stressed: if the strange channels show a general tendency to be underestimated by QCDF, there is the striking exception of the  $\bar{s}ss$  channels which agree very well with QCDF and make the case for charming penguins diagrams rather difficult.

## VI. CONCLUSION

We have made a global fit according to QCD factorization of published experimental data concerning charmless  $B \rightarrow PV$  decays including  $CP$  asymmetries. We have only excluded from the fit the channels containing the  $\eta'$  meson. Our conclusion is that it is impossible to reach a good fit. As can be seen in scenario 1 of Table V, the reason for this failure is that the branching ratios for the strange channels are predicted to be significantly smaller than experiment except for the  $B \rightarrow \phi K$  channels, and in Table VI it can be seen that the direct  $CP$  asymmetry of  $\bar{B} \rightarrow \rho^+ \pi^-$  is predicted very small while experiment gives it very large but only two sigmas from zero. Not only is the ‘‘goodness of the fit’’ smaller than 0.1%, but the fitted parameters show a tendency to evade the allowed domain of QCD factorization. One might wonder if we were not too strict in imposing the same scale  $\mu$  in all terms since the value of  $\mu$ , representing the effect of unknown higher order corrections, could be different in different classes of channels.<sup>2</sup> We have performed several tests relaxing this unicity of  $\mu$  and concluded that it affected very little the outcome of our fit.

<sup>2</sup>We thank Gerhard Buchalla for raising this question.

For the sake of comparison with the authors of Ref. [36] we have tried a fit without the channels containing a  $K^*$ . The result improves significantly. The only lesson we can receive from this is that one must look carefully at the evolution of the experimental results, many of them being recent, before drawing a final conclusion.

Both the small predicted branching ratios of the strange channels and the small predicted direct  $CP$  asymmetries in the nonstrange channels could be blamed on too small  $P$  amplitudes with too small “strong phases” relatively to the  $T$  amplitudes. We have therefore tried the addition of two “charming-penguin”-diagram-inspired long-distance complex amplitudes combined, in order to make the model predictive enough, with exact flavor-SU(3) symmetry and the OZI rule. This fit is better than the pure QCDF one: with a goodness of fit of about 8% the model is not excluded by experiment. But the parameters show again a tendency to reach the limits of the allowed domain and the best fit gives rather small value to the long-distance contribution. The latter fact is presumably due to the  $B \rightarrow \phi K$  which are well predicted by QCDF and thus deliver a message which contradicts the other strange channels. This seems to be the reason of the moderate success of our “charming-penguin”-diagram-inspired model.

Altogether, the present situation is unpleasant. QCDF seems to be unable to comply to experiment. QCDF implemented by an *ad hoc* long-distance model is not fully convincing. No clear hint at the origin of this problem is provided by the total set of experimental data. PQCD, also called  $k_T$  factorization, would predict larger direct  $CP$  asymmetries, but we do not know if their sign would fit experiment either if an overall agreement of the branching ratios with data can be achieved.

Maybe, however, the coming experimental data will move enough to resolve, at least partly, this discrepancy. We would like to insist on the crucial importance of direct  $CP$  asymmetries in nonstrange channels. If they confirm the tendency to be large, this would make the case for QCDF really difficult.

Finally we do not know yet the answer to our initial question: are we in a good position to study the unitarity-triangle angle  $\alpha$  from indirect  $CP$  asymmetries thanks to small penguin diagrams. If experimental data evolve so as to provide a better support to QCDF, one could become bold enough to use it in estimating  $\alpha$  and this would reduce the errors. Else, only model-independent bounds [46] could be used but they are not very constraining in part because of discrete ambiguities.

*Note added in proof.* Since this paper was submitted, one of us (P.-F.G.) has finalized a new experimental estimate of the  $\rightarrow \rho\pi$  and  $B \rightarrow \rho K$  channels for the Babar Collaboration and redone the fits presented in this paper [47]. As a result, the confidence level raises to 1% for the QCDF and drops to 3% for the charming penguins.

#### ACKNOWLEDGMENTS

We are grateful to Gerhard Buchalla for useful discussions on various aspects of this work. A.S.S. would like to thank PROCOPE 2002 and DESY for financial support. We thank André Gaidot, Alain Le Yaouanc, Lluís Oliver, Jean-Claude Raynal, and Christophe Yèche for several enlightening discussions which initiated this work as well as Sébastien Descotes at a later stage.

#### APPENDIX A: THE DECAY AMPLITUDES FOR $B \rightarrow PV$

Following Ref. [32], we give the decay amplitudes for the following  $B \rightarrow PV$  decay processes.

##### 1. $b \rightarrow d$ processes

$$\mathcal{A}(\bar{B}^0 \rightarrow \rho^- \pi^+) = \frac{G_F}{\sqrt{2}} m_B^2 f_\rho F_1^{B \rightarrow \pi}(m_\rho^2) \{ \lambda'_u a_1 + (\lambda'_u + \lambda'_c) [a_4 + a_{10}] \}, \quad (\text{A1})$$

$$\mathcal{A}(\bar{B}^0 \rightarrow \rho^+ \pi^-) = \frac{G_F}{\sqrt{2}} m_B^2 f_\pi A_0^{B \rightarrow \rho}(m_\pi^2) \{ \lambda'_u a_1 + (\lambda'_u + \lambda'_c) [a_4 + a_{10} - r_\chi^\pi (a_6 + a_8)] \}, \quad (\text{A2})$$

$$\begin{aligned} \mathcal{A}(\bar{B}^0 \rightarrow \pi^0 \rho^0) = & -\frac{G_F}{2\sqrt{2}} m_B^2 \left( f_\pi A_0^{B \rightarrow \rho}(m_\pi^2) \left\{ \lambda'_u a_2 - (\lambda'_u + \lambda'_c) \left[ a_4 - \frac{1}{2} a_{10} - r_\chi^\pi \left( a_6 - \frac{1}{2} a_8 \right) + \frac{3}{2} (a_7 - a_9) \right] \right\} \right. \\ & \left. + f_\rho F_1^{B \rightarrow \pi}(m_\rho^2) \left\{ \lambda'_u a_2 - (\lambda'_u + \lambda'_c) \left( a_4 - \frac{1}{2} a_{10} - \frac{3}{2} (a_7 + a_9) \right) \right\} \right), \quad (\text{A3}) \end{aligned}$$

$$\begin{aligned} \mathcal{A}(B^- \rightarrow \pi^- \rho^0) &= \frac{G_F}{2} m_B^2 \left[ f_\pi A_0^{B \rightarrow \rho} (m_\pi^2) \{ \lambda'_u a_1 + (\lambda'_u + \lambda'_c) [a_4 + a_{10} - r_\chi^\pi (a_6 + a_8)] \} \right. \\ &\quad \left. + f_\rho F_1^{B \rightarrow \pi} (m_\rho^2) \left\{ \lambda'_u a_2 + (\lambda'_u + \lambda'_c) \left( -a_4 + \frac{1}{2} a_{10} + \frac{3}{2} (a_7 + a_9) \right) \right\} \right], \end{aligned} \quad (\text{A4})$$

$$\begin{aligned} \mathcal{A}(B^- \rightarrow \rho^- \pi^0) &= \frac{G_F}{2} m_B^2 \left( f_\pi A_0^{B \rightarrow \rho} (m_\pi^2) \left\{ \lambda'_u a_2 + (\lambda'_u + \lambda'_c) \left[ -a_4 + \frac{1}{2} a_{10} - r_\chi^\pi \left( -a_6 + \frac{1}{2} a_8 \right) + \frac{3}{2} (a_9 - a_7) \right] \right\} \right. \\ &\quad \left. + f_\rho F_1^{B \rightarrow \pi} (m_\rho^2) \{ \lambda'_u a_1 + (\lambda'_u + \lambda'_c) [a_4 + a_{10}] \} \right), \end{aligned} \quad (\text{A5})$$

$$\begin{aligned} \mathcal{A}(B^- \rightarrow \pi^- \omega) &= \frac{G_F}{2} m_B^2 \left( f_\pi A_0^{B \rightarrow \omega} (m_\pi^2) \{ \lambda'_u a_1 + (\lambda'_u + \lambda'_c) [a_4 + a_{10} - r_\chi^\pi (a_6 + a_8)] \} \right. \\ &\quad \left. + f_\omega F_1^{B \rightarrow \pi} (m_\omega^2) \left\{ \lambda'_u a_2 + (\lambda'_u + \lambda'_c) \left[ a_4 + 2(a_3 + a_5) + \frac{1}{2} (a_7 + a_9 - a_{10}) \right] \right\} \right), \end{aligned} \quad (\text{A6})$$

## 2. $b \rightarrow s$ processes

$$\mathcal{A}(\bar{B}^0 \rightarrow K^{*-} \pi^+) = \frac{G_F}{\sqrt{2}} m_B^2 f_{K^*} F_1^{B \rightarrow \pi} (m_{K^*}^2) \{ \lambda_u a_1 + (\lambda_u + \lambda_c) [a_4 + a_{10}] \}, \quad (\text{A7})$$

$$\mathcal{A}(\bar{B}^0 \rightarrow K^- \rho^+) = \frac{G_F}{\sqrt{2}} m_B^2 f_K A_0^{B \rightarrow \rho} (m_K^2) \{ \lambda_u a_1 + (\lambda_u + \lambda_c) [a_4 + a_{10} - r_\chi^K (a_6 + a_8)] \}, \quad (\text{A8})$$

$$\begin{aligned} \mathcal{A}(\bar{B}^0 \rightarrow \bar{K}^0 \rho^0) &= \frac{G_F}{2} m_B^2 \left\{ f_K A_0^{B \rightarrow \rho} (m_{K^0}^2) (-\lambda_u - \lambda_c) \left[ a_4 - \frac{1}{2} a_{10} - r_\chi^K \left( a_6 - \frac{1}{2} a_8 \right) \right] \right. \\ &\quad \left. + f_\rho F_1^{B \rightarrow K} (m_\rho^2) \left[ \lambda_u a_2 + (\lambda_u + \lambda_c) \times \frac{3}{2} (a_9 + a_7) \right] \right\}, \end{aligned} \quad (\text{A9})$$

$$\begin{aligned} \mathcal{A}(B^- \rightarrow K^{*-} \pi^0) &= \frac{G_F}{2} m_B^2 \left[ f_\pi A_0^{B \rightarrow K^*} (m_\pi^2) \left\{ \lambda_u a_2 + (\lambda_u + \lambda_c) \times \frac{3}{2} (a_9 - a_7) \right\} \right. \\ &\quad \left. + f_{K^*} F_1^{B \rightarrow \pi} (m_{K^*}^2) \{ \lambda_u a_1 + (\lambda_u + \lambda_c) (a_4 + a_{10}) \} \right], \end{aligned} \quad (\text{A10})$$

$$\begin{aligned} \mathcal{A}(B^- \rightarrow K^- \rho^0) &= \frac{G_F}{2} m_B^2 \left[ f_K A_0^{B \rightarrow \rho} (m_K^2) \{ \lambda_u a_1 + (\lambda_u + \lambda_c) [a_4 + a_{10} - r_\chi^K (a_6 + a_8)] \} \right. \\ &\quad \left. + f_\rho F_1^{B \rightarrow K} (m_\rho^2) \left\{ \lambda_u a_2 + (\lambda_u + \lambda_c) \times \frac{3}{2} (a_9 + a_7) \right\} \right], \end{aligned} \quad (\text{A11})$$

$$\begin{aligned} \mathcal{A}(\bar{B}^0 \rightarrow \bar{K}^0 \omega) &= \frac{G_F}{2} m_B^2 \left( f_K A_0^{B \rightarrow \omega} (m_{K^0}^2) (\lambda_u + \lambda_c) \left[ a_4 - \frac{1}{2} a_{10} - r_\chi^K \left( a_6 - \frac{1}{2} a_8 \right) \right] \right. \\ &\quad \left. + f_\omega F_1^{B \rightarrow K} (m_\omega^2) \left\{ \lambda_u a_2 + (\lambda_u + \lambda_c) \left[ 2(a_3 + a_5) + \frac{1}{2} (a_9 + a_7) \right] \right\} \right), \end{aligned} \quad (\text{A12})$$

$$\begin{aligned} \mathcal{A}(B^- \rightarrow K^- \omega) &= \frac{G_F}{2} m_B^2 \left[ f_K A_0^{B \rightarrow \omega} (m_K^2) \{ \lambda_u a_1 + (\lambda_u + \lambda_c) [a_4 + a_{10} - r_\chi^K (a_6 + a_8)] \} \right. \\ &\quad \left. + f_\omega F_1^{B \rightarrow K} (m_\omega^2) \left\{ \lambda_u a_2 + (\lambda_u + \lambda_c) \left[ 2(a_3 + a_5) + \frac{1}{2} (a_9 + a_7) \right] \right\} \right], \end{aligned} \quad (\text{A13})$$

$$\begin{aligned}
\mathcal{A}(B^- \rightarrow K^{*-} \eta^{(\prime)}) &= \frac{G_F}{\sqrt{2}} m_B^2 \left[ f_{K^{(\prime)}} F_1^{B \rightarrow \eta^{(\prime)}}(m_K^2) \{ \lambda_u a_1 + (\lambda_u + \lambda_c)(a_4 + a_{10}) \} + f_{\eta^{(\prime)}}^u A_0^{B \rightarrow K^*}(m_{\eta^{(\prime)}}^2) \right. \\
&\quad \times \left( \lambda_u a_2 + \lambda_c a_2 \frac{f_{\eta^{(\prime)}}^c}{f_{\eta^{(\prime)}}^u} + (\lambda_u + \lambda_c) \left\{ 2(a_3 - a_5) + \frac{1}{2}(a_9 - a_7) + r_\chi^{\eta^{(\prime)}} \left( a_6 - \frac{1}{2} a_8 \right) \right. \right. \\
&\quad \left. \left. + (a_3 - a_5 + a_9 - a_7) \frac{f_{\eta^{(\prime)}}^c}{f_{\eta^{(\prime)}}^u} + \left[ a_3 - a_5 - \frac{1}{2}(a_9 - a_7) + a_4 - \frac{1}{2} a_{10} - r_\chi^{\eta^{(\prime)}} \left( a_6 - \frac{1}{2} a_8 \right) \right] \frac{f_{\eta^{(\prime)}}^s}{f_{\eta^{(\prime)}}^u} \right\} \right) \left. \right], \tag{A14}
\end{aligned}$$

$$\begin{aligned}
\mathcal{A}(\bar{B}^0 \rightarrow \bar{K}^{*0} \eta^{(\prime)}) &= \frac{G_F}{\sqrt{2}} m_B^2 \left[ f_{K^{(\prime)}} F_1^{B \rightarrow \eta^{(\prime)}}(m_K^2) (\lambda_u + \lambda_c) \left[ a_4 - \frac{1}{2} a_{10} \right] + f_{\eta^{(\prime)}}^u A_0^{B \rightarrow K^*}(m_{\eta^{(\prime)}}^2) \right. \\
&\quad \times \left( \lambda_u a_2 + \lambda_c a_2 \frac{f_{\eta^{(\prime)}}^c}{f_{\eta^{(\prime)}}^u} + (\lambda_u + \lambda_c) \left\{ 2(a_3 - a_5) + \frac{1}{2}(a_9 - a_7) + r_\chi^{\eta^{(\prime)}} \left( a_6 - \frac{1}{2} a_8 \right) \right. \right. \\
&\quad \left. \left. + (a_3 - a_5 + a_9 - a_7) \frac{f_{\eta^{(\prime)}}^c}{f_{\eta^{(\prime)}}^u} + \left[ a_3 - a_5 - \frac{1}{2}(a_9 - a_7) + a_4 - \frac{1}{2} a_{10} - r_\chi^{\eta^{(\prime)}} \left( a_6 - \frac{1}{2} a_8 \right) \right] \frac{f_{\eta^{(\prime)}}^s}{f_{\eta^{(\prime)}}^u} \right\} \right) \left. \right], \tag{A15}
\end{aligned}$$

with  $r_\chi^{\eta^{(\prime)}} = 2m_{\eta^{(\prime)}}^2 / (m_b + m_s)(m_s + m_s)$ .

### 3. Pure penguin processes

$$\mathcal{A}(B^- \rightarrow \pi^- \bar{K}^{*0}) = \frac{G_F}{\sqrt{2}} m_B^2 f_{K^*} F_1^{B \rightarrow \pi}(m_{K^*}^2) (\lambda_u + \lambda_c) \left[ a_4 - \frac{1}{2} a_{10} \right], \tag{A16}$$

$$\mathcal{A}(B^- \rightarrow \rho^- \bar{K}^0) = \frac{G_F}{\sqrt{2}} m_B^2 f_{K^*} A_0^{B \rightarrow \rho}(m_{K^*}^2) (\lambda_u + \lambda_c) \left[ a_4 - \frac{1}{2} a_{10} - r_\chi^K \left( a_6 - \frac{1}{2} a_8 \right) \right], \tag{A17}$$

$$\mathcal{A}(B^- \rightarrow K^- K^{*0}) = \frac{G_F}{\sqrt{2}} m_B^2 f_{K^*} F_1^{B \rightarrow K}(m_{K^*}^2) (\lambda_u' + \lambda_c') \left[ a_4 - \frac{1}{2} a_{10} \right], \tag{A18}$$

$$\mathcal{A}(B^- \rightarrow K^{*-} K^0) = \frac{G_F}{\sqrt{2}} m_B^2 f_{K^*} A_0^{B \rightarrow K^*}(m_{K^*}^2) (\lambda_u' + \lambda_c') \left[ a_4 - \frac{1}{2} a_{10} - r_\chi^K \left( a_6 - \frac{1}{2} a_8 \right) \right], \tag{A19}$$

$$\mathcal{A}(B^- \rightarrow \pi^- \phi) = -\frac{G_F}{2} m_B^2 f_\phi F_1^{B \rightarrow \pi}(m_\phi^2) (\lambda_u' + \lambda_c') \left[ a_3 + a_5 - \frac{1}{2}(a_7 + a_9) \right], \tag{A20}$$

$$\begin{aligned}
\mathcal{A}(B^- \rightarrow K^- \phi) &= \mathcal{A}(\bar{B}^0 \rightarrow \bar{K}^0 \phi) \\
&= \frac{G_F}{\sqrt{2}} m_B^2 f_\phi F_1^{B \rightarrow K}(m_\phi^2) (\lambda_u + \lambda_c) \left[ a_3 + a_4 + a_5 - \frac{1}{2}(a_7 + a_9 + a_{10}) \right]. \tag{A21}
\end{aligned}$$

### APPENDIX B: THE ANNIHILATION AMPLITUDES FOR $B \rightarrow PV$

We give in this section the following annihilation amplitudes for  $B \rightarrow PV$  already given in Ref. [35] but with different notations.

**1.  $b \rightarrow d$  processes**

$$\begin{aligned} \mathcal{A}^a(\bar{B}^0 \rightarrow \pi^- \rho^+) &= \frac{G_F}{\sqrt{2}} f_B f_\pi f_\rho \left\{ \lambda'_u b_1(\rho^+, \pi^-) + (\lambda'_u + \lambda'_c) \left[ b_3(\pi^-, \rho^+) + b_4(\rho^+, \pi^-) + b_4(\pi^-, \rho^+) \right. \right. \\ &\quad \left. \left. - \frac{1}{2} b_3^{ew}(\pi^-, \rho^+) + b_4^{ew}(\rho^+, \pi^-) - \frac{1}{2} b_4^{ew}(\pi^-, \rho^+) \right] \right\}, \end{aligned} \quad (\text{B1})$$

$$\begin{aligned} \mathcal{A}^a(\bar{B}^0 \rightarrow \pi^+ \rho^-) &= \frac{G_F}{\sqrt{2}} f_B f_\pi f_\rho \left\{ \lambda'_u b_1(\pi^+, \rho^-) + (\lambda'_u + \lambda'_c) \left[ b_3(\rho^-, \pi^+) + b_4(\pi^+, \rho^-) + b_4(\rho^-, \pi^+) \right. \right. \\ &\quad \left. \left. - \frac{1}{2} b_3^{ew}(\rho^-, \pi^+) + b_4^{ew}(\pi^+, \rho^-) - \frac{1}{2} b_4^{ew}(\rho^-, \pi^+) \right] \right\}, \end{aligned} \quad (\text{B2})$$

$$\begin{aligned} \mathcal{A}^a(\bar{B}^0 \rightarrow \pi^0 \rho^0) &= \frac{G_F}{2\sqrt{2}} f_B f_\pi f_\rho \left\{ \lambda'_u [b_1(\rho^0, \pi^0) + b_1(\pi^0, \rho^0)] + (\lambda'_u + \lambda'_c) \left[ b_3(\rho^0, \pi^0) + b_3(\pi^0, \rho^0) + 2b_4(\pi^0, \rho^0) \right. \right. \\ &\quad \left. \left. + 2b_4(\rho^0, \pi^0) + \frac{1}{2} [-b_3^{ew}(\rho^0, \pi^0) - b_3^{ew}(\pi^0, \rho^0) + b_4^{ew}(\pi^0, \rho^0) + b_4^{ew}(\rho^0, \pi^0)] \right] \right\}, \end{aligned} \quad (\text{B3})$$

$$\begin{aligned} \mathcal{A}^a(B^- \rightarrow \pi^- \rho^0) &= \frac{G_F}{2} f_B f_\pi f_\rho \{ \lambda'_u [b_2(\pi^-, \rho^0) - b_2(\rho^0, \pi^-)] + (\lambda'_u + \lambda'_c) [b_3(\pi^-, \rho^0) - b_3(\rho^0, \pi^-) \\ &\quad + b_3^{ew}(\pi^-, \rho^0) - b_3^{ew}(\rho^0, \pi^-)] \}, \end{aligned} \quad (\text{B4})$$

$$\begin{aligned} \mathcal{A}^a(B^- \rightarrow \pi^0 \rho^-) &= \frac{G_F}{2} f_B f_\pi f_\rho \{ \lambda'_u [b_2(\rho^-, \pi^0) - b_2(\pi^0, \rho^-)] + (\lambda'_u + \lambda'_c) [b_3(\rho^-, \pi^0) - b_3(\pi^0, \rho^-) \\ &\quad + b_3^{ew}(\rho^-, \pi^0) - b_3^{ew}(\pi^0, \rho^-)] \}, \end{aligned} \quad (\text{B5})$$

$$\begin{aligned} \mathcal{A}^a(B^- \rightarrow \pi^- \omega) &= \frac{G_F}{2} f_B f_\pi f_\omega \{ \lambda'_u [b_2(\pi^-, \omega) + b_2(\omega, \pi^-)] + (\lambda'_u + \lambda'_c) [b_3(\pi^-, \omega) + b_3(\omega, \pi^-) \\ &\quad + b_3^{ew}(\pi^-, \omega) + b_3^{ew}(\omega, \pi^-)] \}, \end{aligned} \quad (\text{B6})$$

**2.  $b \rightarrow s$  processes**

$$\mathcal{A}^a(\bar{B}^0 \rightarrow \pi^+ K^{*-}) = \frac{G_F}{\sqrt{2}} f_B f_\pi f_{K^*} \left\{ (\lambda_u + \lambda_c) \left[ b_3(K^{*-}, \pi^+) - \frac{1}{2} b_3^{ew}(K^{*-}, \pi^+) \right] \right\}, \quad (\text{B7})$$

$$\mathcal{A}^a(\bar{B}^0 \rightarrow K^- \rho^+) = \frac{G_F}{\sqrt{2}} f_B f_K f_\rho \left\{ (\lambda_u + \lambda_c) \left[ b_3(K^-, \rho^+) - \frac{1}{2} b_3^{ew}(K^-, \rho^+) \right] \right\}, \quad (\text{B8})$$

$$\mathcal{A}^a(\bar{B}^0 \rightarrow \bar{K}^0 \rho^0) = -\frac{G_F}{2} f_B f_K f_\rho \left\{ (\lambda_u + \lambda_c) \left[ b_3(\bar{K}^0, \rho^0) - \frac{1}{2} b_3^{ew}(\bar{K}^0, \rho^0) \right] \right\}, \quad (\text{B9})$$

$$\mathcal{A}^a(\bar{B}^0 \rightarrow \bar{K}^0 \omega) = \frac{G_F}{2} f_B f_K f_\omega \left\{ (\lambda_u + \lambda_c) \left[ b_3(\bar{K}^0, \omega) - \frac{1}{2} b_3^{ew}(\bar{K}^0, \omega) \right] \right\}, \quad (\text{B10})$$

$$\mathcal{A}^a(B^- \rightarrow K^- \omega) = \frac{G_F}{2} f_B f_K f_\omega \{ \lambda_u b_2(K^-, \omega) + (\lambda_u + \lambda_c) [b_3(K^-, \omega) + b_3^{ew}(K^-, \omega)] \}. \quad (\text{B11})$$

$$\mathcal{A}^a(B^- \rightarrow \pi^0 K^{*-}) = \frac{G_F}{2} f_B f_\pi f_{K^*} \{ \lambda_u b_2(K^{*-}, \pi^0) + (\lambda_u + \lambda_c) [b_3(K^{*-}, \pi^0) + b_3^{ew}(K^{*-}, \pi^0)] \}, \quad (\text{B12})$$

$$\mathcal{A}^a(B^- \rightarrow K^- \rho^0) = \frac{G_F}{2} f_B f_K f_\rho \{ \lambda_u b_2(K^-, \rho^0) + (\lambda_u + \lambda_c) [b_3(K^-, \rho^0) + b_3^{ew}(K^-, \rho^0)] \}, \quad (\text{B13})$$

$$\begin{aligned} \mathcal{A}^a(\bar{B}^0 \rightarrow \eta^{(\prime)} \bar{K}^{*0}) &= \frac{G_F}{\sqrt{2}} f_B f_{\eta^{(\prime)}}^u f_{K^*} \left\{ (\lambda_u + \lambda_c) \left[ b_3(\bar{K}^{*0}, \eta^{(\prime)}) - \frac{1}{2} b_3^{ew}(\bar{K}^{*0}, \eta^{(\prime)}) \right. \right. \\ &\quad \left. \left. + \frac{f_{\eta^{(\prime)}}^s}{f_{\eta^{(\prime)}}^u} \left( b_3(\eta^{(\prime)}, \bar{K}^{*0}) - \frac{1}{2} b_3^{ew}(\eta^{(\prime)}, \bar{K}^{*0}) \right) \right] \right\}, \end{aligned} \quad (\text{B14})$$

$$\begin{aligned} \mathcal{A}^a(B^- \rightarrow \eta^{(\prime)} K^{*-}) &= \frac{G_F}{\sqrt{2}} f_B f_{\eta^{(\prime)}}^u f_{K^*} \left\{ \lambda_u \left[ b_2(K^{*-}, \eta^{(\prime)}) + \frac{f_{\eta^{(\prime)}}^s}{f_{\eta^{(\prime)}}^u} b_2(\eta^{(\prime)}, K^{*-}) \right] \right. \\ &\quad \left. + (\lambda_u + \lambda_c) \left[ b_3(K^{*-}, \eta^{(\prime)}) + b_3^{ew}(K^{*-}, \eta^{(\prime)}) + \frac{f_{\eta^{(\prime)}}^s}{f_{\eta^{(\prime)}}^u} (b_3(\eta^{(\prime)}, K^{*-}) + b_3^{ew}(\eta^{(\prime)}, K^{*-})) \right] \right\}. \end{aligned} \quad (\text{B15})$$

### 3. Pure penguin diagram processes

$$\mathcal{A}^a(B^- \rightarrow \pi^- \bar{K}^{*0}) = \frac{G_F}{\sqrt{2}} f_B f_\pi f_{K^*} \{ \lambda_u b_2(\bar{K}^{*0}, \pi^-) + (\lambda_u + \lambda_c) [b_3(\bar{K}^{*0}, \pi^-) + b_3^{ew}(\bar{K}^{*0}, \pi^-)] \}. \quad (\text{B16})$$

$$\mathcal{A}^a(B^- \rightarrow \bar{K}^0 \rho^-) = \frac{G_F}{\sqrt{2}} f_B f_K f_\rho \{ \lambda_u b_2(\bar{K}^0, \rho^-) + (\lambda_u + \lambda_c) [b_3(\bar{K}^0, \rho^-) + b_3^{ew}(\bar{K}^0, \rho^-)] \}, \quad (\text{B17})$$

$$\mathcal{A}^a(B^- \rightarrow K^- K^{*0}) = \frac{G_F}{\sqrt{2}} f_B f_K f_{K^*} \{ \lambda_u' b_2(K^{*0}, K^-) + (\lambda_u' + \lambda_c') [b_3(K^{*0}, K^-) + b_3^{ew}(K^{*0}, K^-)] \}, \quad (\text{B18})$$

$$\mathcal{A}^a(B^- \rightarrow K^0 K^{*-}) = \frac{G_F}{\sqrt{2}} f_B f_K f_{K^*} \{ \lambda_u' b_2(K^0, K^{*-}) + (\lambda_u' + \lambda_c') [b_3(K^0, K^{*-}) + b_3^{ew}(K^0, K^{*-})] \}, \quad (\text{B19})$$

$$\mathcal{A}^a(B^- \rightarrow \pi^- \phi) = \mathcal{A}^a(\bar{B}^0 \rightarrow \pi^0 \phi) = 0. \quad (\text{B20})$$

$$\mathcal{A}^a(B^- \rightarrow K^- \phi) = \frac{G_F}{\sqrt{2}} f_B f_K f_\phi \{ \lambda_u b_2(\phi, K^-) + (\lambda_u + \lambda_c) [b_3(\phi, K^-) + b_3^{ew}(\phi, K^-)] \}, \quad (\text{B21})$$

$$\mathcal{A}^a(\bar{B}^0 \rightarrow \bar{K}^0 \phi) = \frac{G_F}{\sqrt{2}} f_B f_K f_\phi \left\{ (\lambda_u + \lambda_c) \left[ b_3(\phi, \bar{K}^0) - \frac{1}{2} b_3^{ew}(\phi, \bar{K}^0) \right] \right\}. \quad (\text{B22})$$

- [1] BABAR Collaboration, B. Aubert *et al.*, hep-ex/0107058.  
 [2] BABAR Collaboration, Thomas Schietinger, in Proceedings of the Lake Louise Winter Institute on Fundamental Interactions, Alberta, Canada, 2001, hep-ex/0105019.  
 [3] BABAR Collaboration, B. Aubert *et al.*, Phys. Rev. Lett. **87**, 151801 (2001).  
 [4] BABAR Collaboration, B. Aubert *et al.*, hep-ex/0107037.  
 [5] BABAR Collaboration, B. Aubert *et al.*, hep-ex/0109007.  
 [6] BABAR Collaboration, B. Aubert *et al.*, hep-ex/0109006.  
 [7] BABAR Collaboration, B. Aubert *et al.*, Phys. Rev. D **65**, 051101(R) (2002).

- [8] BABAR Collaboration, B. Aubert *et al.*, hep-ex/0206053.  
 [9] BABAR Collaboration, B. Aubert *et al.*, hep-ex/0207068.  
 [10] BABAR Collaboration, B. Aubert *et al.*, Phys. Rev. Lett. **87**, 221802 (2001); BABAR Collaboration, A. Bevan, talk presented at ICHEP2002, Amsterdam, Holland, 2002; BABAR Collaboration, P. Bloom, talk at Meeting of the Division of Particles and Fields, American Physical Society, Williamsburg, Virginia, 2002.  
 [11] Belle Collaboration, B. C. K. Casey *et al.*, Phys. Rev. D **66**, 092002 (2002); Belle Collaboration, R. S. Lu *et al.*, Phys. Rev. Lett. **89**, 191801 (2002); Belle Collaboration, A. Gordon *et al.*,

- Phys. Lett. B **542**, 183 (2002); Belle Collaboration, A. Garmash *et al.*, Phys. Rev. D **65**, 092005 (2002); Belle Collaboration, P. Chang, talk presented at ICHEP2002, Amsterdam, Holland, 2002; Belle Collaboration, K. F. Chen, talk presented at ICHEP2002, Amsterdam, Holland, 2002; Belle Collaboration, H. C. Huang, talk at 37th Rencontres de Moriond on Electroweak Interactions and Unified Theories, Les Arcs, France, 2002, to appear in the proceedings.
- [12] Belle Collaboration, A. Bozek, in Proceedings of the 4th International Conference on B Physics and  $CP$  Violation, Ise-Shima, Japan, 2001, hep-ex/0104041.
- [13] Belle Collaboration, K. Abe *et al.* in Proceedings of the XX International Symposium on Lepton and Photon Interactions at High Energies, 2001, Rome, Italy, Report No. Belle-CONF-0115, 2001.
- [14] Belle Collaboration, H. Tajima, Int. J. Mod. Phys. A **17**, 2967 (2002).
- [15] Belle Collaboration, K. Abe *et al.*, Phys. Rev. D **65**, 092005 (2002).
- [16] CLEO Collaboration, R. A. Briere *et al.*, Phys. Rev. Lett. **86**, 3718 (2001).
- [17] CLEO Collaboration, C. P. Jessop *et al.*, Phys. Rev. Lett. **85**, 2881 (2000).
- [18] CLEO Collaboration, C. P. Jessop *et al.*, hep-ex/9908018.
- [19] CLEO Collaboration, S. J. Richichi *et al.*, Phys. Rev. Lett. **85**, 520 (2000).
- [20] CLEO Collaboration, S. Chen *et al.*, Phys. Rev. Lett. **85**, 525 (2000).
- [21] CLEO Collaboration, D. Cronin-Hennessy *et al.*, Phys. Rev. Lett. **85**, 515 (2000); CLEO Collaboration, E. Eckhart *et al.*, *ibid.* **89**, 251801 (2002).
- [22] M. Beneke, G. Buchalla, M. Neubert, and C. T. Sachrajda, Phys. Rev. Lett. **83**, 1914 (1999); Nucl. Phys. **B591**, 313 (2000).
- [23] M. Beneke, G. Buchalla, M. Neubert, and C. T. Sachrajda, Nucl. Phys. **B606**, 245 (2001).
- [24] C. Isola, M. Ladisa, G. Nardulli, T. N. Pham, and P. Santorelli, Phys. Rev. D **65**, 094005 (2002).
- [25] M. Ciuchini, E. Franco, G. Martinelli, M. Pierini, and L. Silvestrini, Phys. Lett. B **515**, 33 (2001).
- [26] C. W. Chiang, Phys. Rev. D **62**, 014017 (2000).
- [27] M. Ciuchini, R. Contino, E. Franco, G. Martinelli, and L. Silvestrini, Nucl. Phys. **B512**, 3 (1998); **B531**, 656(E) (1998).
- [28] M. Ciuchini, E. Franco, G. Martinelli, and L. Silvestrini, hep-ph/9909530.
- [29] C. Isola, M. Ladisa, G. Nardulli, T. N. Pham, and P. Santorelli, Phys. Rev. D **64**, 014029 (2001).
- [30] M. Ciuchini, E. Franco, G. Martinelli, and L. Silvestrini, Nucl. Phys. **B501**, 271 (1997).
- [31] R. Aleksan, F. Buccella, A. Le Yaouanc, L. Oliver, O. Pene, and J. C. Raynal, Phys. Lett. B **356**, 95 (1995).
- [32] A. Ali, G. Kramer, and C. D. Lü, Phys. Rev. D **58**, 094009 (1998); **59**, 014005 (1999).
- [33] G. Kramer, W. F. Palmer, and H. Simma, Z. Phys. C **66**, 429 (1995).
- [34] M. Z. Yang and Y. D. Yang, Phys. Rev. D **62**, 114019 (2000).
- [35] D. s. Du, H. j. Gong, J. f. Sun, D. s. Yang, and G. h. Zhu, Phys. Rev. D **65**, 094025 (2002); **66**, 079904(E) (2002).
- [36] D. s. Du, J. f. Sun, D. s. Yang, and G. h. Zhu, Phys. Rev. D **67**, 014023 (2003).
- [37] C. H. Chen, Y. Y. Keum, and H. n. Li, Phys. Rev. D **64**, 112002 (2001).
- [38] Y. Y. Keum, hep-ph/0210127.
- [39] W. N. Cottingham, H. Mehrban, and I. B. Whittingham, J. Phys. G **28**, 2843 (2002).
- [40] M. Nagashima and H. n. Li, Phys. Rev. D **67**, 034001 (2003); Y. Y. Keum and H. n. Li, *ibid.* **63**, 074006 (2001).
- [41] Y. Y. Keum, H. N. Li, and A. I. Sanda, Phys. Lett. B **504**, 6 (2001); Phys. Rev. D **63**, 054008 (2001).
- [42] C. D. Lü, K. Ukai, and M. Z. Yang, Phys. Rev. D **63**, 074009 (2001).
- [43] Particle Data Group Collaboration, K. Hagiwara *et al.*, Phys. Rev. D **66**, 010001 (2002).
- [44] F. James, computer code MINUIT, CERN Program Library D506.
- [45] P. Ball and V. M. Braun, Phys. Rev. D **58**, 094016 (1998).
- [46] Jérôme Charles, Ph.D. thesis, Université Paris-Sud, 1999; see <http://tel.ccsd.cnrs.fr/>
- [47] Pierre-François Giraud, Ph.D. thesis, Université Paris-Sud, 2003; see <http://tel.ccsd.cnrs.fr/>